Department of Neuroanatomy
Theoretical Medicine and Biosciences
Faculty of Medicine
Saarland University, Homburg (Saar)

Decreased Expression of the EAAT5 Glutamate Transporter at Photoreceptor Synapses in Early, Pre-Clinical Experimental Autoimmune Encephalomyelitis, a Mouse Model of Multiple Sclerosis

A thesis submitted to the Faculty of Medicine in fulfilment of the requirements for the degree of

Dr. Med.

of the Medical Faculty of Saarland University

2025

By

Ali El Samad

born on 02.11.1994 in Lebanon

Supervisor: Prof. Dr. Frank Schmitz

Declaration

I hereby declare that the M.D. thesis entitled "Decreased Expression of the EAAT5 Glutamate Transporter at Photoreceptor Synapses in Early, Pre-Clinical Experimental Autoimmune Encephalomyelitis, a Mouse Model of Multiple Sclerosis" is a presentation of my original research work. All external sources of information have been acknowledged. No portion of this thesis work has been submitted in support of any other degree or qualification.

Homburg, 21.04.2025

Ali El Samad

Acknowledgements

I would like to express my deep gratitude to Prof. Frank Schmitz for giving me the opportunity to perform my thesis work in his lab.

I would like to thank all my colleagues and friends for their continuous support throughout this journey.

I would like to express my gratitude to Julia Jaffal for all her efforts and unconditional support during my thesis.

Special thanks to Dalia Ibrahim and Karin Schwarz for their help and amazing input throughout this journey.

Table of content

Contents

1 SUMMARY

Multiple sclerosis (MS) is a widespread neurological disorder characterized by both neuroinflammatory and neurodegenerative complications. This disease often leads to significant changes in the structural and functional integrity of the brain's white and gray matter. The visual system is highly vulnerable to disruptions associated with MS progression. One suspected factor in MS pathogenesis is glutamate excitotoxicity. This study is focused on the EAAT5 (SLC1A7) glutamate transporter, which is crucial for glutamate regulation at the synapses and is positioned near the active zones of photoreceptor ribbon synapses.

In my thesis, i used the experimental autoimmune encephalomyelitis (EAE) mouse model to examine how changes in EAAT5 might influence the structure and functionality of photoreceptor ribbon synapses in MS. I performed qualitative and quantitative techniques, including immunofluorescence microscopy and Western blot analyses, to measure EAAT5 expression and its localization at day 9 post-immunization, during the pre-clinical stage of EAE.

My results indicate a significant decline in EAAT5 at the photoreceptor synapses in EAE-afflicted retinas as compared to controls, observed starting from day 9 nine post-immunization. This decline was confirmed through Western blot analysis showing reduced EAAT5 protein levels. Such early impairments in glutamate transport suggest a potential involvement of EAAT5 in the synaptic abnormalities seen in MS.

This investigation underscores the role of EAAT5 in maintaining synaptic balance and proposed EAAT5 imbalance as potential mechanisms contribute to MS related neurodegenerative and neuroinflammatory manifestations. These findings contribute to a deeper understanding of the molecular underpinnings of MS and may inform future therapeutic strategies targeting synaptic dysfunction in this disease.

1 ZUSAMMENFASSUNG

Multiple Sklerose (MS) ist eine weit verbreitete neurologische Erkrankung, die sowohl durch neuroinflammatorische als auch neurodegenerative Komplikationen gekennzeichnet ist. Diese Krankheit führt häufig zu erheblichen Veränderungen in der strukturellen und funktionellen Integrität der weißen und grauen Substanz des Gehirns. Besonders anfällig für Störungen, die mit dem Fortschreiten der MS einhergehen, ist das visuelle System. Ein vermuteter Faktor in der Pathogenese der MS ist die Glutamat-Exzitotoxizität. Die vorliegende Studie konzentriert sich auf den EAAT5 (SLC1A7) Glutamat-Transporter, der eine entscheidende Rolle bei der Regulation von Glutamat an den Synapsen spielt und sich in der Nähe der aktiven Zonen der Photorezeptor-Ribbon-Synapsen befindet. In meiner Dissertation habe ich das experimentelle Modell der autoimmunen Enzephalomyelitis (EAE) bei Mäusen verwendet, um zu untersuchen, wie Veränderungen in EAAT5 die Struktur und Funktionalität von Photorezeptor-Ribbon-Synapsen bei MS beeinflussen könnten. Ich setzte qualitative und quantitative Methoden ein, darunter Immunfluoreszenzmikroskopie und Western-Blot-Analysen, um die Expression und Lokalisation von EAAT5 am neunten Tag nach der Immunisierung während der präklinischen Phase der EAE zu messen.

Meine Ergebnisse zeigen einen signifikanten Rückgang von EAAT5 an den Photorezeptor-Synapsen in von EAE betroffenen Retinas im Vergleich zu Kontrollen, beginnend ab dem neunten Tag nach der Immunisierung. Dieser Rückgang wurde durch Western-Blot-Analysen bestätigt, die eine reduzierte EAAT5-Proteinexpression zeigten. Solche frühen Beeinträchtigungen im Glutamattransport deuten auf eine mögliche Beteiligung von EAAT5 an den synaptischen Anomalien bei MS hin.

Diese Untersuchung unterstreicht die Rolle von EAAT5 bei der Aufrechterhaltung des synaptischen Gleichgewichts und schlägt ein Ungleichgewicht von EAAT5 als möglichen Mechanismus vor, der zu den neurodegenerativen und neuroinflammatorischen Manifestationen der MS beiträgt. Diese Erkenntnisse vertiefen unser Verständnis der molekularen Grundlagen der MS und könnten zukünftige therapeutische Strategien zur Zielsetzung der synaptischen Dysfunktion bei dieser Krankheit informieren.

2 Introduction

2.1 Multiple Sclerosis (MS)

Multiple sclerosis (MS) is a chronic, immune-mediated disease of the central nervous system (CNS) characterized by inflammation, demyelination, and axonal degeneration (DOBSON, GIOVANNONI, 2019; WARD, GOLDMAN, 2022). It predominantly affects young adults, with a higher prevalence among women. The pathological hallmark of MS involves the formation of plaques in the brain and spinal cord, where myelin—the protective layer around nerve fibers—is damaged. This demyelination leads to impaired conduction of electrical signals along affected neurons, contributing to the wide range of clinical manifestations (KORN, 2008). MS is categorized into different subtypes based on its progression: relapsing-remitting MS is the most common form at onset, characterized by episodes of neurological dysfunction followed by periods of partial or complete recovery, whereas progressive forms, including primary progressive MS and secondary progressive MS (SPMS), are associated with a steady accumulation of disability (COMPSTON, COLES, 2008; GAKIS et al., 2024; THOMPSON et al., 2018).
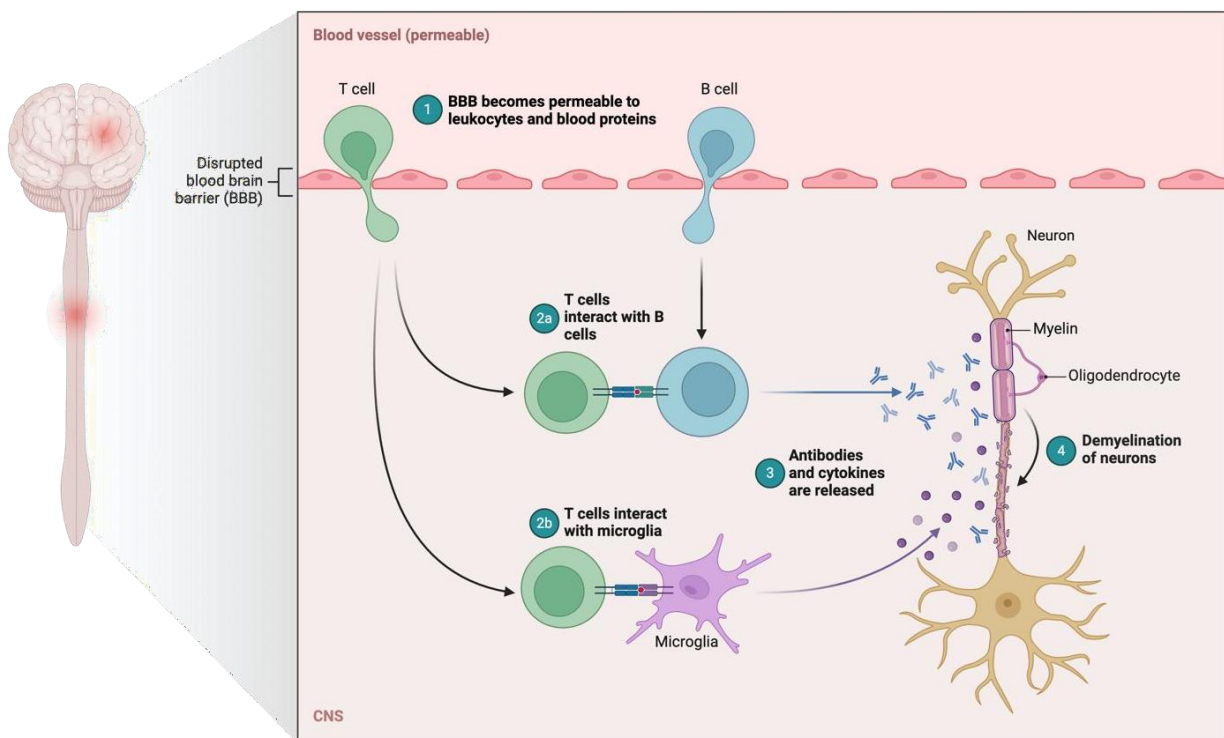

Figure 1. Pathogenesis of Multiple Sclerosis. This illustration delineates three potential mechanisms by which circulating autoantibodies may contribute to the pathogenesis of multiple sclerosis. 1) Under

inflammatory conditions, such as enhanced permeability of the blood-brain barrier precipitated by encephalitogenic T lymphocytes, antibodies that penetrate the brain may exert pathogenic effects. 2) These antibodies can potentially induce vascular damage and inflammatory lesions within the CNS through processes involving complement-dependent cytotoxicity or antibody-dependent cellular cytotoxicity, mediated by Fc receptors on microglia and macrophages. 3) Autoreactive B cells might infiltrate the brain, leading to elevated intrathecal antibody production. Moreover, antibodies adhering to the surface of target cells can cause direct damage or modify the functionality of these cells, leading to demyelination. Additionally, antibodies may facilitate demyelination indirectly by activating autoreactive T cells, or microglia and macrophages.

Adapted from (STERLING, MATTHEWS, 2005)

The clinical consequences of MS are highly variable and depend on the location and extent of CNS damage. Symptoms may include motor weakness, spasticity, sensory disturbances such as numbness and tingling, visual impairment (often due to optic neuritis), and coordination difficulties. Fatigue is one of the most commonly reported and disabling symptoms (GAKIS et al., 2024; LUBLIN, 2005). Cognitive dysfunction is observed in approximately 40–70% of patients, often manifesting as memory impairment, reduced processing speed, and executive function deficits (BENEDICT et al., 2020). Emotional disturbances, such as depression and anxiety, are prevalent and significantly impact the quality of life. In advanced stages, MS may result in severe physical disability, with affected individuals requiring mobility aids or full-time care (RAIMO et al., 2021). The extent of disability is frequently assessed using the Expanded Disability Status Scale (EDSS), which quantifies the impact on motor and non-motor functions (KAUR et al., 2012; WASIMUDDIN et al., 2018).

The pathological processes underlying MS involve both inflammatory and neurodegenerative mechanisms. Early in the disease, inflammation predominates, driven by activated immune cells, including T lymphocytes, B cells, and macrophages, which breach the blood-brain barrier and target myelin (MAHAD et al., 2015). Over time, neurodegenerative processes, including axonal loss and gliosis, become more prominent, contributing to irreversible neurological deficits. Lesions typically occur in the white matter regions of the CNS, such as the periventricular areas, spinal cord, and optic nerves, although grey matter involvement is also increasingly recognized. Advanced imaging techniques, particularly magnetic resonance imaging (MRI), play a crucial role in diagnosing MS and monitoring disease progression by detecting these lesions (KINDLER et al., 2013; MEY et al., 2023; THOMPSON et al., 2018).

MS is a lifelong disease with no definitive cure, but disease-modifying therapies have significantly improved outcomes by reducing the frequency and severity of relapses and slowing disability progression (HAUSER, CREE, 2020). These therapies target the immune-mediated mechanisms underlying MS and include agents such as interferons, monoclonal antibodies, and oral immunomodulators. However, treatment efficacy varies among individuals, and the long-term

management of MS requires a multidisciplinary approach to address its physical, cognitive, and emotional consequences (HAUSER, CREE, 2020; SANGER et al., 2010; WASIMUDDIN et al., 2018). With this understanding of MS as a chronic CNS condition, we now shift our focus to the role of glutamate and its transporters, key players in maintaining neural homeostasis and their implications in MS pathology (KOSTIC et al., 2013).

2.2 Glutamate and Glutamate Transporters

Given the importance of understanding MS's complex mechanisms, it is essential to delve into the role of glutamate, the primary excitatory neurotransmitter in the CNS, and the transporters that regulate its extracellular concentration. These transporters are critical to maintaining neural homeostasis and protecting against excitotoxicity, a hallmark of MS pathology (KOSTIC et al., 2013).

Glutamate is the primary excitatory neurotransmitter in the CNS, where it is essential for synaptic transmission, neuronal communication, and plasticity (BROSNAN, BROSNAN, 2013; ZHOU, DANBOLT, 2014). It plays a crucial role in cognitive processes such as learning and memory, as well as sensory perception. During synaptic transmission, glutamate is released from presynaptic neurons into the synaptic cleft, where it activates ionotropic receptors, including α-amino-3-hydroxy-5-methyl-4-isoxazolepropionic acid (AMPA), N-Methyl-D-aspartic acid (NMDA), and kainate receptors, as well as metabotropic glutamate receptors on postsynaptic neurons (BROSNAN, BROSNAN, 2013; MAEZAWA et al., 2004; ZHOU, DANBOLT, 2014). This activation triggers downstream signaling cascades involving calcium influx, which drives synaptic plasticity and intracellular signaling pathways.

While glutamate is indispensable for normal CNS function, its activity must be tightly regulated. Excessive extracellular glutamate overstimulates receptors, particularly NMDA receptors, leading to excitotoxicity—a pathological process associated with calcium overload, oxidative stress, and mitochondrial dysfunction (AMBROGINI et al., 2019; BADING et al., 1995; LAU, TYMIANSKI, 2010; NICHOLLS, 2004). These processes result in neuronal damage or apoptosis, contributing to the loss of neural connectivity and impaired CNS function (LAU, TYMIANSKI, 2010; SHAW, INCE, 1997). To prevent excitotoxicity and maintain synaptic homeostasis, the CNS relies on excitatory amino acid transporters (EAATs) to clear glutamate from the synaptic cleft (GREEN et al., 2021). EAATs actively transport glutamate into surrounding glial cells or presynaptic terminals, ensuring that extracellular concentrations remain within physiological limits. The EAAT family includes five subtypes—EAAT1 to EAAT5—each with unique properties and distinct tissue distributions, enabling precise regulation of glutamate levels in different regions of the CNS.

EAAT1 and EAAT2 are predominantly expressed in astrocytes, where they account for the majority of glutamate uptake in the CNS (YI, HAZELL, 2006). EAAT2 alone is responsible for approximately 90% of glutamate clearance and plays a pivotal role in preventing excitotoxicity during high neuronal activity. EAAT1 is also expressed in glial cells but is particularly enriched in the cerebellum, contributing to glutamate regulation in this region. EAAT3, found in neurons, supports intracellular recycling of glutamate for metabolic processes such as glutathione synthesis, which is critical for maintaining the antioxidative capacity of neurons. EAAT4 is localized to cerebellar Purkinje cells, where it combines glutamate transport with ion channel-like properties to modulate cerebellar function and maintain motor coordination (RODRIGUEZ-CAMPUZANO, ORTEGA, 2021; SHIGERI et al., 2004; VANDENBERG, RYAN, 2013).

EAAT5, the most specialized member of the EAAT family, is primarily expressed in the CNS and is highly concentrated at synapses in regions requiring dynamic regulation of glutamate. Unlike other EAATs, EAAT5 functions as both a high-affinity glutamate transporter and a chloride channel (THORESON, CHHUNCHHA, 2023). This dual functionality allows it to hyperpolarize presynaptic membranes, thereby modulating neurotransmitter release in response to synaptic activity. EAAT5's chloride conductance property provides additional control over synaptic responses, ensuring that glutamate release is precisely calibrated to the demands of neural signaling (GEHLEN et al., 2021; TANG et al., 2022).

The unique localization of EAAT5 at presynaptic terminals highlights its importance in maintaining synaptic integrity. By rapidly clearing glutamate from the synaptic cleft, EAAT5 prevents the overstimulation of ionotropic receptors such as NMDA and AMPA receptors, preserving the precision of excitatory signaling. Its role extends beyond glutamate uptake; the chloride channel function contributes to the fine-tuning of synaptic transmission, making it indispensable for regions where synaptic activity fluctuates rapidly (PALMER et al., 2003; WERSINGER et al., 2006).

In addition to its role in glutamate clearance, EAAT5 participates in light adaptation and sensory processing by regulating neurotransmitter dynamics in response to changes in synaptic demand. This makes it particularly valuable in neural circuits that require continuous or graded neurotransmitter release, such as those in sensory systems. EAAT5's ability to maintain synaptic homeostasis under varying activity levels underscores its significance in overall CNS function (MAGI et al., 2019; MALIK, WILLNOW, 2019; PALMER et al., 2003).

The structural and functional properties of EAAT5 also contribute to its efficiency. Its high affinity for glutamate ensures rapid uptake even at low extracellular concentrations, while its dual transporter-channel activity adds a layer of complexity to its regulation of synaptic dynamics. This specialization distinguishes EAAT5 from other EAATs and positions it as a critical regulator of excitatory signaling.

Building on the understanding of glutamate and its transporters, it becomes evident how their dysregulation during MS contributes to the progression of the disease. Let us now explore this critical dysfunction in greater detail (LIANG et al., 2008; MAGI et al., 2019).
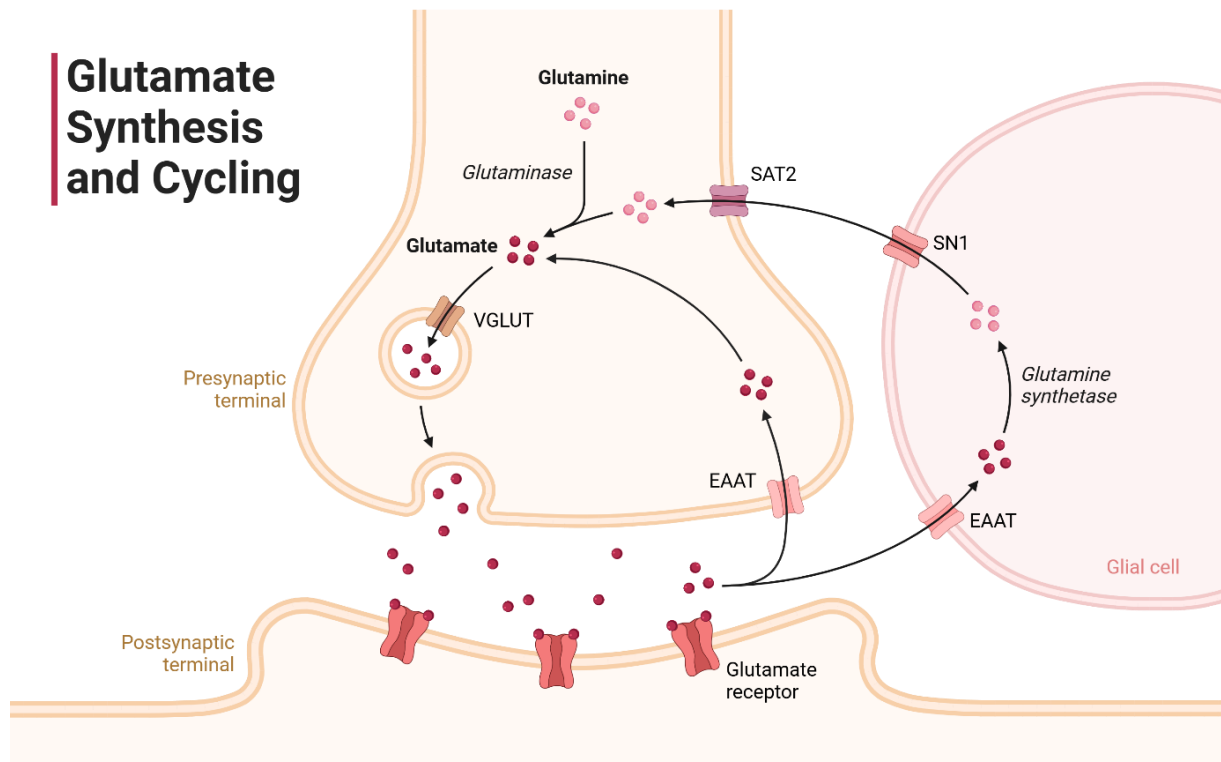
Figure 2. Glutamate synthesis and Glutamate Transporters. The diagram outlines the function of excitatory amino acid transporters (EAATs) in the removal of glutamate (Glu) from the synaptic cleft. Glutamate enters glial cells and is metabolically converted into glutamine (Gln) by glutamine synthetase. Following this conversion, glutamine is transported out of the glial cells via sodium-coupled neutral amino acid transporters (SNATs). Neurons then take up glutamine through SNAT1 and SNAT2, where it is converted back into glutamate by phosphate-activated glutaminase. This regenerated glutamate is subsequently loaded into synaptic vesicles by vesicular glutamate transporters (VGLUTs) and released into the synaptic cleft, thus supporting further excitatory neurotransmission. Adapted from (MACHTENS et al., 2015).

2.3 Glutamate Transporters Dysregulation During MS

Building on the understanding of glutamate and its transporters, it is critical to examine how their dysregulation contributes to MS pathology. The dysfunction of glutamate transporters is a key factor in the excitotoxic processes driving neurodegeneration in MS (SATTLER, ROTHSTEIN, 2006; STOJANOVIC et al., 2014).

The pathological mechanisms underlying MS are complex and involve both neuroinflammatory and neurodegenerative processes. Among these, excitotoxicity, driven by excessive extracellular glutamate, plays a pivotal role in the progression of neuronal and synaptic damage in MS (SHELDON, ROBINSON, 2007). Elevated glutamate levels have been consistently observed in the CNS of MS patients, particularly in regions of active inflammation and demyelination. This accumulation of glutamate reflects a disruption in the delicate balance between glutamate release and uptake, a process heavily reliant on the activity of EAATs(NEWCOMBE et al., 2008; SATTLER, ROTHSTEIN, 2006; STOJANOVIC et al., 2014).

EAAT dysfunction has been implicated in the failure to clear excess glutamate in MS, leading to prolonged stimulation of ionotropic glutamate receptors, increased intracellular calcium levels, and the activation of downstream neurotoxic pathways (MITOSEK-SZEWCZYK et al., 2008). Inflammatory cytokines such as tumor necrosis factor-alpha (TNF-α) and interleukin-1 beta (IL-1β), which are abundant in MS lesions, have been shown to downregulate EAAT expression and activity, exacerbating glutamate-mediated excitotoxicity. This disruption not only damages neurons but also affects glial cells, further impairing glutamate homeostasis and perpetuating the neuroinflammatory cycle (INOUE et al., 1996; MCCARTHY et al., 2012; PALLE et al., 2017; SUTTON et al., 2006).

EAAT5, as a specialized glutamate transporter, plays a significant role in modulating synaptic glutamate dynamics, particularly in regions of high synaptic activity. In MS, reduced expression or functional impairment of EAAT5 has been identified in experimental autoimmune encephalomyelitis (EAE) models, an established animal model for MS. This reduction is associated with increased extracellular glutamate and enhanced susceptibility to excitotoxic damage. EAAT5's unique ability to regulate glutamate levels and its additional chloride channel activity make it a critical player in limiting excitotoxicity under inflammatory conditions. Its dysfunction exacerbates synaptic and neuronal degeneration, particularly in areas of high synaptic turnover, such as optic pathways and other sensory regions (RAJDA et al., 2017; THORESON, CHHUNCHHA, 2023).

Moreover, the interplay between glutamate dysregulation and immune-mediated damage in MS further underscores the importance of EAAT5. During neuroinflammation, EAAT5's protective mechanisms are compromised, leading to enhanced glutamate release and impaired reuptake at synaptic sites. This creates a toxic microenvironment that accelerates neuronal loss and contributes to the progression of disability in MS. The loss of EAAT5 function not only impairs synaptic precision but also diminishes the capacity of neurons to adapt to the increased metabolic and excitatory demands imposed by chronic inflammation (WERNER et al., 2000, 2001).

Therapeutic strategies targeting EAAT5 may offer potential benefits in managing MS-related excitotoxicity. Enhancing EAAT5 expression or mimicking its dual transporter and chloride channel functions could help restore glutamate homeostasis, reduce synaptic damage, and protect neurons from inflammatory insults. Although current therapies primarily target immune modulation, integrating

strategies that address excitotoxicity through EAAT5 could complement existing approaches and improve outcomes in MS patients.

With the role of glutamate transporter dysfunction in MS pathology established, we now turn to the anatomy of the mammalian eye, which provides a basis for understanding how MS affects visual pathways.

2.4 Anatomy of the Mammalian Eye

With the understanding of MS and its effects on glutamate transporters, it is important to explore the anatomy of the mammalian eye. This knowledge lays the foundation for understanding the impact of MS on visual pathways. The mammalian eye is a highly specialized organ designed to capture light and convert it into meaningful neural signals, ultimately forming the perception of vision. Its anatomy is divided into three principal layers, each serving distinct functional roles.

The outermost layer, composed of the cornea and sclera, acts as a protective shield for the delicate internal components. The cornea, a transparent and highly refractive structure, serves as the primary medium for bending incoming light toward the retina. It works in conjunction with the sclera, the opaque, fibrous "white" of the eye, which maintains the eye's shape and protects it from external damage. The middle layer includes the iris, ciliary body, and choroid. The iris regulates light entry by controlling the pupil size, expanding in low light and constricting in bright conditions. Behind the iris lies the ciliary body, which adjusts the lens's shape to focus images at various distances, a process known as accommodation. The choroid, rich in blood vessels, nourishes both the retina and the outer layers of the eye, ensuring optimal cellular function. The innermost layer, the retina, is where light detection and signal transduction occur. Despite its location, the retina is an integral part of the CNS, extending directly from the brain. It captures light through specialized photoreceptors and initiates a complex cascade of biochemical reactions to convert visual stimuli into electrochemical signals. These signals are transmitted to the brain via the optic nerve for further processing (AGATHOCLEOUS, HARRIS, 2009; CEPKO et al., 1996; DAGHSNI, ALDIRI, 2021).

Anatomy of the Human Eye
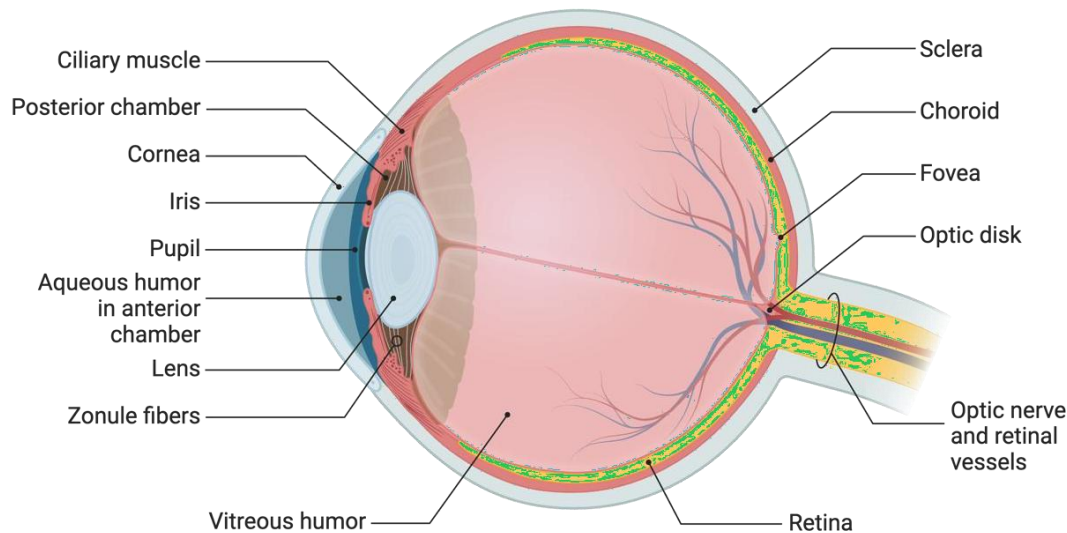
Figure 3. Anatomy of mammalian eye. This is an illustration that describes the anatomical part of the human eye. Adapted from (BAEK et al., 2024).

Light enters the eye through the cornea and is further refracted by the crystalline lens, which fine-tunes the focus onto the retina. This intricate process enables the retina to detect subtle variations in light intensity, color, and movement, laying the foundation for detailed visual perception. To fully appreciate the relationship between MS and visual dysfunction, it is essential to delve deeper into the structure and function of the retina, the primary site of light detection and neural processing in the eye.

## 2.5 Structure and Function of the Retina

Building on the anatomy of the eye, we now focus on the retina, the neural structure responsible for capturing and processing light. Understanding its organization and functionality is crucial for analyzing how MS affects visual pathways (1868). The retina, a layered structure critical to vision, comprises two main components: the retinal pigment epithelium (RPE) and the neural retina. The RPE forms a monolayer of pigmented cells that lies adjacent to the choroid. It plays a pivotal role in photoreceptor maintenance by absorbing excess light, recycling photoreceptor outer segments, and regulating nutrient exchange. The RPE also helps maintain the blood-retina barrier, which protects the neural retina from harmful substances (1868; HOON et al., 2014).

The **neural retina** consists of five primary neuronal cell types: photoreceptors, bipolar cells, ganglion cells, horizontal cells, and amacrine cells. These cells are arranged in distinct layers, reflecting their specialized roles in visual processing. The photoreceptors (rods and cones) are located in the outermost

layer. Rods are highly sensitive to low light and are primarily responsible for scotopic (night) vision, while cones are sensitive to bright light and enable photopic (color) vision. These cells initiate phototransduction, a biochemical cascade that converts light into electrical signals (DE MORAES, 2013; KELTS, 2010; REESE, 2011; ZHU et al., 2023).

Bipolar cells act as intermediaries, transmitting signals from photoreceptors to ganglion cells, which are the retina's output neurons. The axons of ganglion cells converge to form the optic nerve, carrying visual information to the brain's visual cortex. Horizontal and amacrine cells mediate lateral interactions, enhancing contrast sensitivity and refining spatial and temporal aspects of visual stimuli. Supportive Müller glial cells, spanning the entire retinal thickness, maintain structural integrity and regulate the ionic environment. Additionally, astrocytes and microglia contribute to the retina's immune defense and homeostasis. Having established the structural complexity of the retina, it is essential to explore the synaptic pathways within this organ to understand how visual information is transmitted and integrated (AGUIRRE et al., 2016; BRINGMANN, WIEDEMANN, 2012; REESE, 2011).
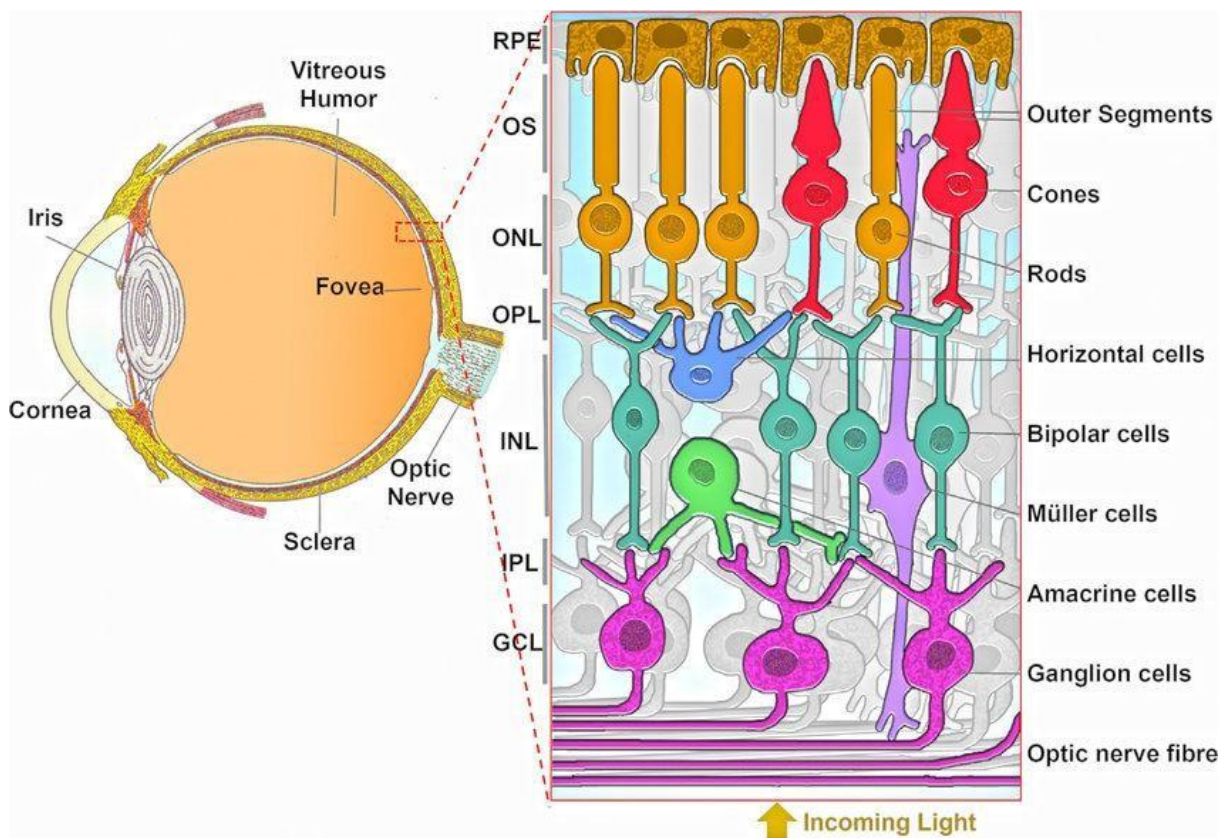
Figure 4 . Structure of human retina. Situated at the innermost layer of the eye, the retina comprises an intricate network of neurons, interneurons, and ganglion cells. It is systematically organized into five specific layers: the Ganglion Cell Layer (GCL), Inner Nuclear Layer (INL), Outer Nuclear Layer (ONL), and the synaptic zones of the Inner Plexiform Layer (IPL) and Outer Plexiform Layer (OPL). The retina's photoreceptors, rods and cones, initiate phototransduction by transforming light into electrical signals. This process takes place in the outer segments of the photoreceptors, which are closely associated with the apical microvilli of the Retinal Pigment Epithelium (RPE) cells. The conversion

signals are then propagated to the ganglion cells via bipolar and amacrine cells, ultimately transmitting visual information to the brain through the optic nerve. Adapted from (KARALI, BANFI, 2015)

2.6 Retinal Synaptic Pathways

With an understanding of the structural organization of the retina, we now turn to its synaptic pathways, which facilitate the transmission and integration of visual signals. These pathways play a pivotal role in processing light information and adapting to varying visual demands.

The transmission of visual signals within the retina occurs through specialized synaptic pathways that integrate excitatory and inhibitory inputs. The outer plexiform layer (OPL) and inner plexiform layer (IPL) serve as the primary sites of synaptic interaction. In the OPL, photoreceptors form synapses with bipolar and horizontal cells. Bipolar cells mediate the vertical transmission of signals, while horizontal cells provide lateral inhibition. This lateral interaction enhances visual contrast, allowing for edge detection and image sharpening. The OPL serves as the first site where light signals are modified to emphasize spatial differences, crucial for interpreting fine details in the visual scene (BULDYREV et al., 2012; FURUKAWA et al., 2020; JOHNSON et al., 1999; TIAN, 2004).

In the IPL, bipolar cells transmit signals to ganglion cells, the retina's output neurons, while also interacting with amacrine cells. Amacrine cells play a key role in modulating temporal aspects of visual signals, such as motion detection and adaptation to changes in light intensity. This layer integrates complex spatial and temporal information before relaying it to the brain for further processing. The retina processes light increments and decrements through ON and OFF pathways. ON bipolar cells depolarize in response to increased light, while OFF bipolar cells hyperpolarize in response to decreased light scene (BULDYREV et al., 2012; FURUKAWA et al., 2020; JOHNSON et al., 1999; TIAN, 2004). This separation ensures precise coding of light intensity changes, which is critical for detecting motion and adapting to varying illumination levels (HENDRICKSON, 2016; JOHNSON et al., 1999; O'BRIEN et al., 2003). These synaptic pathways exemplify the intricate coordination required to process visual stimuli efficiently. To delve deeper into this complexity, we now examine the morphology and function of ribbon synapses, which are central to continuous neurotransmitter release in the retina.
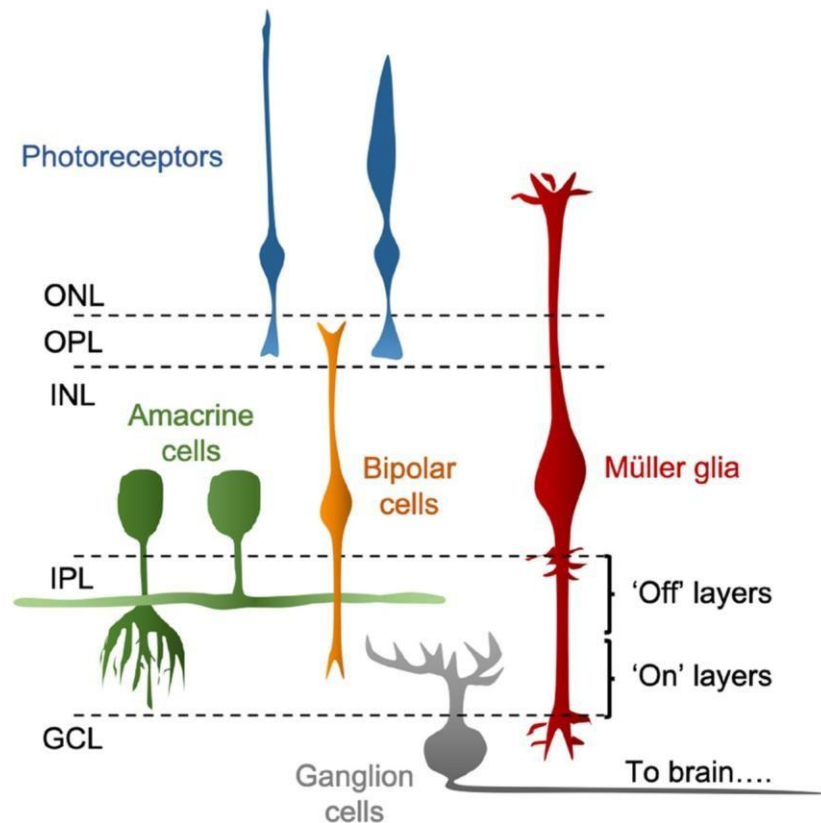
Figure 5 . Retinal Synaptic Pathways. The light is captured by rod and cone photoreceptors, which transform these light signals into neural signals. These light-evoked signals are then transmitted to bipolar cells via glutamatergic synapses located in the OPL. Subsequently, the bipolar cells convey these signals to amacrine and ganglion cells through additional glutamatergic synapses found in the IPL. This network of synaptic connections among bipolar, amacrine, and ganglion cells in the IPL is crucial for feature extraction and the reduction of redundancy in the retinal output. Additionally, Müller glia play a supportive role in maintaining retinal function. Adapted from (GRIMES et al., 2021)

2.6 Morphology and Function of Ribbon Synapses

Building on the understanding of retinal synaptic pathways, it is important to explore ribbon synapses, specialized structures essential for the continuous and rapid transmission of visual information. These synapses are critical to the retina's ability to adapt to the dynamic demands of light and motion processing.

Ribbon synapses, distinct from conventional synapses, are specialized for sustained neurotransmitter release. Found in photoreceptors and bipolar cells, these synapses are characterized by an electron-dense ribbon structure that extends into the cytoplasm from the presynaptic membrane. This ribbon tethers numerous synaptic vesicles, positioning them for rapid and continuous exocytosis. Such a configuration ensures that ribbon synapses can sustain high rates of neurotransmitter release, a feature

indispensable for encoding graded changes in light intensity (BRANDSTATTER et al., 1999; MATTHEWS, FUCHS, 2010; TOM DIECK et al., 2005).

The ribbon is anchored to the active zone by the arciform density, a specialized structure that facilitates vesicle docking and fusion. This configuration allows the vesicles to remain primed for release, enabling the rapid transmission of visual signals. Unlike conventional synapses, which rely on transient bursts of neurotransmitter release, ribbon synapses support continuous exocytosis. This makes them uniquely suited for sensory systems like the retina, where precise and sustained signaling is crucial.

Ribbon synapses are also present in other sensory systems, such as the cochlea, where they support auditory processing. Despite differences in sensory modalities, the physiological role of ribbon synapses remains consistent: to provide a high temporal fidelity in signal transmission (MAGUPALLI et al., 2008; MAXEINER et al., 2016; SCHMITZ, 2009; SCHMITZ et al., 2000; ZANAZZI, MATTHEWS, 2009).

By understanding the unique structure and function of ribbon synapses, we gain insight into how the retina achieves continuous signal transmission under physiological conditions. This knowledge provides a foundation for examining how MS disrupts these systems, particularly within the visual pathways.
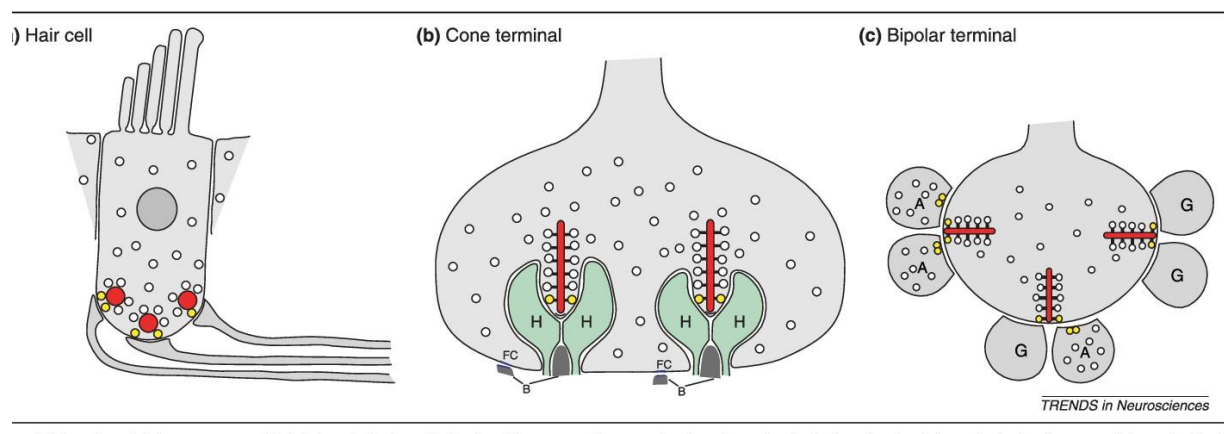
Figure 6 . Morphology and Function of Ribbon Synapses. (A) Hair cells feature ribbons that tether vesicles near the presynaptic membrane, supporting single postsynaptic processes, with around 10–20 ribbons per cell. (B) Cone terminals contain ribbons at invaginations hosting triads of postsynaptic processes (two horizontal cells and one bipolar dendrite), with each cone displaying around 20–50 triads. (C) Bipolar terminals have ribbons connected to postsynaptic processes, which could include ganglion cell dendrites or amacrine processes, with amacrine processes often forming reciprocal synapses. **Adapted from (STERLING, MATTHEWS, 2005)**

2.7 MS and Visual Complications

Having established the foundational anatomy and functionality of the eye and retina, we now focus on how MS impacts the visual system. Visual complications are among the most common and earliest

manifestations of MS, providing a valuable window into understanding the broader neurodegenerative and inflammatory processes associated with the disease.

The visual system is particularly susceptible to MS pathology, with optic neuritis often serving as an early clinical manifestation. This condition is characterized by inflammation of the optic nerve, leading to symptoms such as vision loss, reduced visual acuity, and pain with eye movement. These symptoms reflect the underlying immune-mediated attack on the CNS that defines MS. Damage to the optic nerve and retina has been extensively studied, revealing critical insights into the mechanisms of neurodegeneration in MS. Retinal changes, including degeneration of retinal ganglion cells (RGCs) and disruptions in synaptic structures, are hallmarks of MS-related visual dysfunction. These alterations are driven by inflammatory processes and excitotoxicity, further underscoring the role of immune-mediated damage in MS pathology (COSTELLO, 2016; DHANAPALARATNAM et al., 2022; JASSE et al., 2013; VAN DER FEEN et al., 2022).

EAE, an established animal model of MS, has been instrumental in studying the visual system. EAE studies show that retinal degeneration occurs early in the disease process, even before significant demyelination of the optic nerve. Retinal ganglion cells are particularly vulnerable, with early axonal loss and synaptic disruptions evident in preclinical stages. This suggests that the retina is a site of early neuronal vulnerability in MS and may represent a potential target for therapeutic intervention (CONSTANTINESCU et al., 2011; RAO, SEGAL, 2004; ROBINSON et al., 2014).

Additionally, inflammation-driven alterations in synaptic structure and function within the retina have been documented in MS and EAE. Photoreceptor synapses, which mediate the transmission of visual signals, are significantly affected. Early synaptic changes, including disruptions in synaptic protein expression and neurotransmitter dynamics, precede structural damage to the optic nerve. Glutamate excitotoxicity, a well-documented mechanism in MS, contributes to this synaptic dysfunction by overactivating glutamate receptors, leading to calcium overload and neuronal injury (SCHWARZ, SCHMITZ, 2023).

The molecular mechanisms underlying these early synaptic changes involve a complex interplay between immune cells, glial cells, and neurons. Inflammatory cytokines, such as TNF-α and IL-1β, are upregulated in the retina during MS and EAE, disrupting synaptic integrity and accelerating neurodegeneration. Oxidative stress, mediated by reactive oxygen species (ROS) and nitric oxide, further exacerbates these changes by damaging synaptic proteins and impairing neurotransmitter release. These inflammatory and oxidative stress markers are observed in the retina and other CNS regions affected by MS, highlighting common mechanisms of synaptic and neuronal injury (BARACZKA et al., 2003; BEZZI et al., 2001; ROVARIS et al., 1996).

Given the early synaptic changes observed in MS, targeting these mechanisms could provide a therapeutic avenue. Strategies aimed at mitigating glutamate excitotoxicity or enhancing antioxidant defenses may help preserve synaptic integrity and prevent subsequent neuronal loss. Moreover,

advanced imaging technologies, such as optical coherence tomography (OCT), offer non-invasive methods to monitor retinal changes in vivo, potentially serving as biomarkers for disease activity and therapeutic efficacy (BARACZKA et al., 2003; BEZZI et al., 2001; ROVARIS et al., 1996).

Understanding how MS impacts the visual system underscores the importance of glutamate transporters, particularly EAATs, in preserving synaptic and neuronal integrity. We now turn to the specific role of glutamate transporters in managing visual complications associated with MS.

2.8 Glutamate Transporters' Role in Visual Complications in MS

Building on the understanding of MS-related visual complications, it is critical to explore the potential role of glutamate transporters, EAATs, in managing excitotoxicity and preserving synaptic integrity within the visual system. Dysregulation of these transporters in MS significantly contributes to the progression of visual impairments.

Visual complications in MS, including optic neuritis and retinal degeneration, are closely linked to disruptions in glutamate homeostasis (Is this a hypothesis or a fact? If it is a fact, you need to add the reference. I think you want to say that glutamate transporters likely play an important role. I would re-phrase that chapter accordingly. Glutamate, the primary excitatory neurotransmitter in the CNS, is vital for synaptic signaling in the visual pathways. However, its excessive accumulation during neuroinflammatory conditions such as MS results in excitotoxicity, characterized by overactivation of glutamate receptors, calcium overload, and subsequent neuronal damage. Glutamate transporters, particularly EAAT2 and EAAT5, play a pivotal role in regulating extracellular glutamate levels in the visual system. EAAT2, expressed predominantly in astrocytes along the optic nerve, manages the bulk of glutamate clearance, preventing excessive accumulation at active synapses. Meanwhile, EAAT5, localized presynaptically in retinal neurons, modulates neurotransmitter release and ensures efficient glutamate uptake at photoreceptor and bipolar cell synapses (WERSINGER et al., 2006). Together, these transporters preserve synaptic integrity and prevent excitotoxic damage under physiological conditions (MANDOLESI et al., 2017; MITOSEK-SZEWCZYK et al., 2008; OHGOH et al., 2002; STRUZYNSKA et al., 2005).

In MS, the expression and functionality of these transporters are impaired due to inflammatory processes. Elevated levels of cytokines such as TNF-α and IL-1β in MS lesions downregulate EAAT activity, exacerbating glutamate dysregulation. This is particularly evident in the optic nerve and retinal regions, where high metabolic and synaptic demands make neurons and glial cells highly vulnerable to excitotoxic stress (CENTONZE et al., 2009; MANDOLESI et al., 2015; ROSSI et al., 2014).

EAAT5, with its dual functionality as a glutamate transporter and chloride channel, plays a unique role in synaptic modulation. Its dysfunction in MS has been linked to enhanced susceptibility to excitotoxicity and synaptic instability in high-activity regions such as the retina. Reduced EAAT5

activity contributes to the degeneration of retinal ganglion cell axons and prolonged visual deficits, even after acute episodes of optic neuritis resolve (BOCCUNI, FAIRLESS, 2022). Restoring glutamate transporter function presents a promising avenue for mitigating visual complications in MS. Pharmacological agents that enhance EAAT expression or mimic its functionality could help re-establish glutamate homeostasis and protect synaptic structures from excitotoxic damage. These approaches complement existing immune-modulating therapies and could provide a more comprehensive strategy for preserving visual function in MS (RAJDA et al., 2017; THORESON, CHHUNCHHA, 2023).

In summary, glutamate transporters, particularly EAAT5, are indispensable for maintaining synaptic homeostasis in the visual pathways. Addressing their dysfunction represents a critical step in preventing excitotoxicity and mitigating visual complications in MS.

3 Materials and Methods

3.1 Materials

3.1.1 Antibodies

3.1.1.1 Primary antibodies

Antibody	source	dilution
EAAT5 (immunogen affinity-purified rabbit polyclonal) *	Abcam; Cambridge UK; ab230217	1:200 (IF) 1:500 (WB)
RIBEYE(B) (mouse monoclonal, clone 2D9)	Lab-made	1:1000 (IF)
Actin (mouse monoclonal antibody, clone C4)	Millipore; Molsheim, France; #1501R	1:1000 (IF) 1:1000 (WB)
6xHis, HexaHis-tag (mouse monoclonal antibody, clone 1B7G5)	Proteintech;Planegg-Martinsried, Germany; #66005-1-Ig	1:5000 (WB)

* EAAT5 is a 559 amino acid (aa) long protein in mice (NP_666367.3, GI:1597486091) with a predicted running position at ≈65 kDa in the Western blot (WB) analyses. The affinity-purified rabbit polyclonal EAAT 5 antibody (abcam) was raised against a fusion protein corresponding to amino acid (aa) 100–250 of human EAAT5 (O00341). The specificity of the antibody was verified by a fusion protein that we generated from recombinant synthetic DNA

3.1.1.2 Secondary antibodies

Antibody	Source	Dilution
Chicken anti-rabbit-Alexa488	Invitrogen, Molecular Probes, Karlsruhe, Germany; A-21441	1:1000 (IF)
Donkey anti-rabbit-Alexa488	Invitrogen, Molecular Probes, Karlsruhe, Germany; A-21206	1:1000 (IF)
Donkey anti-mouse-Alexa568	Invitrogen, Molecular Probes, Karlsruhe, Germany; A-10037	1:1000 (IF)

Goat anti-rabbit-horseradish peroxidase (HRP)	Sigma; Taufkirchen, Germany; A6154	1:5000 (WB)
Goat anti-mouse-horseradish peroxidase (HRP)	Sigma; Taufkirchen, Germany; A3673	1:5000 (WB)

3.1.2 Reagents and Chemicals

Name	Company
Acetic acid	Roth
Amido Black	Merck
Benzil	Science Services
Cellulose acetate membrane	GE Healthcare
Cobalt	Merck
Di sodium hydrogen phosphate	Roth
Dimethylsulfoxide	Roth
Ethanol	ZCHL
Formic acid	Merck
gBlock	Integrated DNA Technologies
Gibson Assembly Cloning Kit	New England Biolabs
Incomplete Freund's Adjuvant	Sigma
Low range protein standard Roti marker	Roth
Methanol	Roth
Methyl Butane	Roth
MOG 35-55/ CFA kit	Hooke's Laboratories
Nitrocellulose membrane	Millipore
Non-fat dry milk powder	Supermarket
Paraformaldehyde	Roth
Para-hydroxy Coumarin Acid (PCA)	Roth
Pertussis toxin	List Biological Laboratories
Ponceau S-stain	Roth
Rotiphorese Gel 30 (29% acrylamide, 0.8 % bisacrylamide)	Roth
Sodium azide	Merck
TEMED	Roth
Trichloroacetic acid	Roth
Tween 20	Roth

Whatman filter paper	Roth

3.1.3 Buffers and Solution

Name	Composition
5x phosphate-buffered saline (PBS)	40 g NaCl, 1 g KCl, 7.2 g Na_2HPO_4, 1.2 g KH_2PO4; Make up to 1 litre with dd H_2O
Amidoblack staining solution	0.5% Amidoblack, 45% Methanol, 45% Distilled water, 10% Acetic acid
Amidoblack washing solution	47.5% Methanol, 47.5% Distilled water, 5% Acetic acid
ECL-solution (Chemiluminescence detection system)	1:1 v/v ECL I and ECL II ECL I : 10 ml Tris 1M pH 8.5 1 ml Luminol stock Para-hydroxy Coumarin Acid (PCA) Make volume up to 100 ml with dd H_2O ECL-II: 10 ml Tris 1M pH 8.5 64µl H_2O_2; Make volume up to 100 ml with dd H_2O
imidazole elution buffer	400 mM imidazole 300 mM NaCl, 50 mM NaH_2HPO_4, pH 8.0
imidazole in washing buffer	(300 mM NaCl, 50 mM NaH_2PO_4, pH 8.0).
imidazole lysis buffer	300 mM NaCl, 50 mM NaH_2PO_4, 2.5 mM imidazole, pH 8.0)
MOG 35-55/ Complete Freund's Adjuvant CFA emulsion	200 µg of encephalitogenic MOG35-55 (mouse myelin oligodendrocyte glycoprotein) peptide (MEVGWYRSPFSRVVHLYRNGK; >90% purity, generateded by Dr. Martin Jung, Department ofBiochemistry and Molecular Biology, MedicalSchool Homburg, Saarland University) wasmixed at a concentration of 2 mg/ml in sterile water with an equal volume of complete Freund's adjuvant

	(incomplete Freund's adjuvant, iCFA (Sigma) with 10mg/mlinactivated M. tuberculosis (Fisher Scientific #10218823)).
PBST (1X)	2ml Tween-20 in 900 ml PBS; Make volume up to 1litre with dd H2O
Polyacrylamide 10% running gel	1.5 ml dd H2O, 1.9 ml 1 M Tris pH 8.8, 2.40 ml 30% Acrylamide, 75 µl 10% SDS, 1.5 ml 50%, Glycerol5 µl TEMED, 40 µl 10% APS
Polyacrylamide 7% running gel	2.2 ml dd H_2O,, 1.9 ml 1 M Tris pH 8.8, 1.75 ml 30% Acrylamide, 75 µl 10% SDS, 1.5 ml 50% Glycerol5 µl TEMED, 40 µl 10% APS
Polyacrylamide stacking gel	2.4 ml dd H_2O, 950 µl 1 M Tris pH 6.8, 500 µl 30% Acrylamide, 50 µl 10% SDS, 10 µl TEMED, 50 µl 10% APS
Ponceau S-stain	30 g Trichloroacetic acid, 5g Ponceau; make volume up to 1 litre with dd H2O
PTX solution	200ng of pertussis toxin (PTX) from Bordetella. pertussis (List Biological Laboratories Inc.#180, via Biotrend, Cologne, Germany) was dissolved in 100µl sterile PBS
RIPA lysis buffer composed	150 mM NaCl, 50 mM Tris (pH 7.4), 1% NP-40, 0.5% sodium deoxycholate, 0.1% SDS, and a protease inhibitor cocktail
SDS-loading buffer 4x	1,6 g SDS, 4 ml β-Mercaptoethanol, 2 ml Glycerol, 2 ml 1M Tris pH 7, 4 mg Bromo phenol blue2 ml of ddH2O
SDS-PAGE-electrophoresis buffer	3.03 g Tris, 14.4 g Glycine, 1.0 g SDS; Make volume up to 1 litre with ddH20
Stripping buffer	0.2 M glycine, 0.1% SDS, and adjusted to pH 2.2 Make volume up to 5 litres with dd H2O
Transfer buffer (Western blot)	Tris 15.125 g, Glycine 72.05 g, Methanol 1 litre

3.1.4 Laboratory instruments and consumable materials

Name	Company
Adjustable pipettes	Eppendorf
Autoclave	Tuttnauer Systec 5050ELCV
Axiovert 200, AxioCam MRm (Camera)	Carl Zeiss
Biofuge fresco	Heraeus
Biofuge primo R	Heraeus
Biofuge stratos	Heraeus
Chemidoc XRS system	Bio-Rad
Confocal laser scanning microscope	Nikon
DUO 004B vacuum pump	Arthur-Pfeiffer Vakuumtechnik
Fluorescence microscope	Axiovert 200 M, Carl Zeiss
Freezer -80°C	Heraeus
Hot air oven	Heraeus
Laminar flow model 1,2	Holten
Magnetic stirrer (Complete Set)	Neolab
Overhead rotator	Neolab
pH meter	Inolab
Polyacrylamide gel system	Bio-Rad
Power pack for gel system	GE healthcare
Refrigerated incubator shaker Innova 4320	New Brunswick Scientific
Sterile filtration device	Millipore
Super-resolution structured illumination microscope	Carl Zeiss
Ultra Turrax T8A	IKA Labortechnik;
Ultracut Microtome (UltraCut S)	Leica
Ultrasound Bandelin Sonoplus	Bandelin Electronic, Berlin
Vortex	VWR International

Weighing balance CP64	Sartorius
Western blot transfer apparatus	HOEFER SCIENTIFIC INSTRUMENTS
Wide Field Microscope	Carl Zeiss

3.2 Methods

3.2.1 Induction of Experimental Autoimmune Encephalomyelitis (EAE) in Female Mice

To model MS in preclinical studies, EAE was induced in female C57BL/6J mice aged 10 to 12 weeks and weighing between 20 and 25 grams(DEMBLA et al., 2018; KESHARWANI et al., 2021; ROBINSON et al., 2014). This animal model mirrors the immune-mediated and neuroinflammatory characteristics of MS and provides a valuable platform for investigating disease mechanisms and potential therapeutic strategies. The choice of female mice aligns with the higher prevalence of MS among young women in humans and reflects the standard approach adopted in EAE studies, where female mice are preferentially used due to their heightened susceptibility to autoimmunity (DEMBLA et al., 2018; KESHARWANI et al., 2021; MCCOMBE, GREER, 2022; MUKHERJEE et al., 2020; RAHN et al., 2014; ROBINSON et al., 2014)

Induction of EAE was achieved by immunization with the myelin oligodendrocyte glycoprotein (MOG35–55) peptide, a well-characterized antigen that triggers immune responses against myelin in the CNS. Two approaches were used for immunization: a ready-to-use emulsion from Hooke Laboratories (MOG35–55/CFA Emulsion PTX, containing 1 mg MOG peptide/mL of emulsion) or lab-prepared emulsions. For the latter, the MOG35–55 peptide was dissolved in sterile water at a concentration of 2 mg/mL and emulsified in a one-to-one ratio with complete Freund's adjuvant (CFA). The CFA was prepared by supplementing incomplete Freund's adjuvant with 10 mg/mL of inactivated *Mycobacterium tuberculosis*. Control emulsions contained only CFA, emulsified in an equal ratio with sterile water. A total volume of 200 µL of the prepared emulsion (either MOG/CFA for the experimental group or CFA for the control group) was administered subcutaneously in the axillary and groin regions of each mouse.

To enhance the permeability of the blood-brain barrier and facilitate CNS access for immune cells, pertussis toxin (PTX) from *Bordetella pertussis* was administered intraperitoneally. Each mouse received two injections of 200 ng PTX, the first 60 minutes after the application of the emulsion and the second 16 to 20 hours post-immunization. This dual PTX injection protocol is critical for establishing consistent and robust EAE induction.

The study involved five independent immunization experiments for each of two experimental purposes: immunofluorescence microscopy and Western blot analyses. Each experiment included both experimental animals injected with MOG/CFA emulsion and control animals injected with CFA

emulsion. To ensure unbiased results, animals were randomly assigned to the respective groups and housed together in the same cages to minimize environmental variability. This rigorous experimental design ensures the reproducibility and reliability of findings related to EAE pathophysiology and the evaluation of molecular and cellular outcomes. **EAE induction was done by Karin Schwarz.**

3.2.2 Cloning of pET28a-EAAT5

To facilitate the study of human excitatory amino acid transporter 5 (EAAT5), a cDNA fragment encoding amino acids 100–250 of the protein was successfully cloned into the pET-28a vector using Gibson assembly. This cloning strategy allows for the production of a recombinant EAAT5 fragment, enabling structural and functional analyses of the transporter (GIBSON et al., 2009).

The pET-28a vector was prepared for insertion by linearization through restriction digestion with the enzymes NheI and XhoI. The DNA insert, designed as a synthetic construct (gBlock), was procured from Integrated DNA Technologies. This gBlock contained a sequence encoding amino acids 100–250 of human EAAT5 flanked by 34-nucleotide sequences overlapping the vector at both its 5′ and 3′ ends. These overlapping sequences included the NheI restriction site at the 5′ end and the XhoI restriction site at the 3′ end, facilitating precise alignment during the Gibson assembly reaction.

The design of the gBlock insert incorporated additional functional elements to facilitate downstream protein expression and purification. At the 5′ end, the insert included a STREP-Tag II sequence, immediately followed by the coding sequence for EAAT5 residues 100–250. At the 3′ end, the construct was engineered with vector sequences that ensured proper integration and expression in the host system. The resulting recombinant vector expressed EAAT5 as a fusion protein with the following features: an N-terminal hexa-histidine (His) tag, a thrombin cleavage site, the STREP-Tag II, and a second hexa-His tag at the C-terminal end. These tags facilitate protein purification and allow for flexibility in proteolytic cleavage during downstream processing.

The assembly of the gBlock insert into the linearized pET-28a vector was performed using the Gibson assembly method, a robust and efficient cloning technique. The reaction was carried out in accordance with the manufacturer's protocol using the Gibson Assembly Cloning Kit. This method enabled seamless integration of the insert into the vector by leveraging the overlapping sequences provided in the gBlock design, resulting in a stable and accurate recombinant construct.

The cloned construct was designed to optimize expression and facilitate purification of the EAAT5 fragment in bacterial systems. This strategy provides a reliable platform for studying the structural and functional properties of EAAT5 and exploring its physiological role in glutamate transport and chloride conductance. **Karin Schwarz helped with the cloning of the construct.**

3.2.3 Cloning of pET28a-Cre (Control Protein)

To generate a control protein for experimental applications, a fusion construct comprising the membrane-permeable HIV TAT peptide fused in-frame with Cre recombinase was cloned into the pET-28a expression vector using Gibson assembly. This approach facilitates efficient cloning and expression of the TAT-Cre fusion protein for subsequent experimental studies.

The cloning procedure began with the preparation of the pET-28a vector, which was linearized through restriction digestion using the enzymes NheI and XhoI. This step ensured compatibility with the synthetic DNA insert, enabling precise integration during the Gibson assembly reaction. The insert, a synthetic DNA construct (gBlock), was designed and synthesized by Integrated DNA Technologies. The gBlock included 34-nucleotide sequences at both the 5′ and 3′ ends, overlapping the vector's linearized ends to facilitate seamless assembly.

The 5′ end of the gBlock contained the NheI restriction site, followed by a STREP-Tag II sequence and the coding region for the TAT-Cre fusion protein. This design ensured proper orientation and reading frame alignment during insertion. At the 3′ end, the gBlock included 34 nucleotides of vector-specific sequence, terminating with the XhoI restriction site. These flanking sequences provided a high degree of fidelity and stability during the assembly process.

The resulting recombinant construct expressed TAT-Cre as a fusion protein containing multiple functional elements for ease of purification and processing. The protein included an N-terminal hexa-histidine (His) tag, a thrombin cleavage site, and a STREP-Tag II. These features enable robust purification strategies, including affinity chromatography, while offering flexibility for downstream modifications through site-specific cleavage.

Gibson assembly was performed following the protocol provided by the Gibson Assembly Cloning Kit. This highly efficient method utilizes overlapping DNA sequences to seamlessly assemble the insert and vector into a single recombinant plasmid. The resulting construct was designed to optimize the expression of TAT-Cre in a bacterial system, providing a reliable source of the fusion protein for experimental applications.

This construct allows for the production of a membrane-permeable TAT-Cre protein, which combines the translocation capability of the HIV TAT peptide with the site-specific recombination activity of Cre recombinase. Such a fusion protein is valuable for applications requiring targeted genetic modifications, including studies involving recombinase-mediated gene excision and activation in cellular or in vivo systems. **Karin Schwarz helped with the cloning of the construct.**

3.2.4 Fusion Protein Expression and Purification

The expression and purification of the fusion protein were carried out using a standardized bacterial expression system, specifically employing BL21 T7 Express bacteria. This system is widely used for

the efficient production of recombinant proteins due to its robust growth and high protein expression capabilities (GIBSON et al., 2009).

Transformed bacterial cells were cultured in Luria-Bertani (LB) medium supplemented with 2% glucose to repress basal expression of the T7 promoter and kanamycin (final concentration 10 µg/mL) to maintain plasmid selection. Cultures were incubated at 37 °C with shaking until they reached an optical density at 600 nm (OD600) of 0.8, indicating logarithmic growth and readiness for protein induction. At this point, the expression of the fusion protein was induced by adding isopropyl β-D-1-thiogalactopyranoside (IPTG) to a final concentration of 0.1 mM. Induction was continued for 5 hours at room temperature (RT) to allow sufficient protein production while minimizing the formation of inclusion bodies.

Following induction, bacterial cells were harvested by centrifugation and washed several times with ice-cold PBS to remove residual culture medium and contaminants. The resulting bacterial pellet was resuspended in imidazole lysis buffer, which was supplemented with lysozyme at a concentration of 1 mg/mL to facilitate cell wall digestion. After 30 minutes of incubation on ice to ensure complete enzymatic lysis, the bacterial suspension was subjected to sonication to disrupt the cells and release the fusion protein. The lysate was then cleared by centrifugation at $10,000 \times$ g for 30 minutes at 4 °C to remove cellular debris.

The clarified lysate was incubated overnight with Ni-NTA agarose resin at 4 °C on an overhead rotator, allowing the hexa-histidine (His) tag on the fusion protein to bind to the nickel ions immobilized on the matrix. The ratio of 1 mL of Ni-NTA resin to 500 mL of bacterial culture was used to ensure efficient binding. The lysate-resin mixture was subsequently loaded onto a column, and the flow-through was collected for analysis using SDS-PAGE to monitor protein recovery and evaluate binding efficiency.

To remove nonspecifically bound proteins, the column was washed sequentially with increasing concentrations of imidazole in washing buffer. The washing steps included buffers containing 10 mM, 20 mM, and 250 mM imidazole. These stepwise washes ensured that weakly bound impurities were removed while retaining the fusion protein bound to the Ni-NTA resin.

The bound fusion protein was eluted from the resin by applying 6 mL of imidazole elution buffer. The eluate was collected in 0.5 mL fractions to enable precise identification of the protein-enriched fractions. Subsequent analysis by SDS-PAGE and Western blotting confirmed the enrichment of the EAAT5 fusion protein in fractions 8 to 10. These fractions were pooled and prepared for downstream applications, ensuring high purity and functionality of the recombinant protein.

This protocol highlights the combination of optimized expression conditions and affinity purification strategies for the production of high-quality fusion proteins suitable for biochemical and structural analyses.

3.2.5 Pre-Absorption of EAAT5 Antibody for Immunolabeling Experiments

To confirm the specificity of the EAAT5 antibody used in immunolabeling studies, pre-absorption blocking experiments were conducted. These experiments ensure that the observed immunosignals are specific to the target protein and not the result of cross-reactivity or nonspecific binding.

The working dilution of the EAAT5 antibody was first optimized to 1:200, corresponding to an antibody protein concentration of approximately 167 nM. To validate antibody specificity, the EAAT5 antibody was incubated with the EAAT5 blocking fusion protein (the antigen against which the antibody was raised) or an unrelated fusion protein (HexaHIS-tagged Cre recombinase) in separate experimental and control tubes. Each tube contained the EAAT5 antibody mixed with the respective fusion protein at a molar ratio of 5:1. The mixtures were incubated overnight at 4 °C on a rotator to allow adequate interaction between the antibody and the fusion proteins.

Following the incubation period, both tubes were centrifuged at 30,000 rpm for 5 minutes using a Biofuge Stratos centrifuge to pellet any antigen-antibody complexes. The resulting supernatants, containing unbound antibody, were collected and used for subsequent immunostaining experiments.

Semi-thin sections were processed for co-immunolabeling to compare the immunoreactivity of EAAT5 antibody under experimental and control conditions. One section was incubated with a combination of the EAAT5 antibody, pre-absorbed with the EAAT5 fusion protein, and a mouse monoclonal antibody against RIBEYE (clone 2D9). This setup served as the experimental condition. A parallel section was immunostained with the EAAT5 antibody pre-absorbed with the unrelated HexaHIS-tagged Cre fusion protein, along with the RIBEYE antibody, acting as the control. The RIBEYE immunosignal served as a reference to evaluate EAAT5 antibody specificity. Both incubations were carried out overnight at 4 °C to ensure adequate binding of the primary antibodies to their respective targets.

After incubation, the sections were washed thoroughly with PBS to remove any unbound primary antibodies then incubated for 2 hours at room temperature with fluorescently conjugated secondary antibodies. Binding of the EAAT5 rabbit polyclonal antibody was detected using donkey anti-rabbit immunoglobulins conjugated to Alexa Fluor 488, while binding of the mouse monoclonal RIBEYE antibody (clone 2D9) was with donkey anti-mouse immunoglobulins conjugated to Alexa Fluor 568 (see Table 2) (DEMBLA et al., 2018; KESHARWANI et al., 2021; MUKHERJEE et al., 2020; SHANKHWAR et al., 2022; SUIWAL et al., 2022; WAHL et al., 2013).

Following secondary antibody incubation, the sections were washed five times (5 minutes per wash) with PBS to eliminate excess secondary antibodies and subsequently mounted in n-propyl gallate (NPG) antifade solution, which preserves fluorescence signals during imaging, as previously described (DEMBLA et al., 2018; DEMBLA et al., 2014; GIBSON et al., 2009; RAHN et al., 2014; SCHMITZ et al., 2000; WAHL et al., 2016). Negative control incubations were performed to assess background fluorescence. These controls involved identical incubation steps but omitted the primary antibody to evaluate potential nonspecific fluorescence signals, including autofluorescence. This rigorous protocol

ensured the specificity of EAAT5 antibody labeling and provided reliable immunofluorescence data for subsequent analysis. **This was done with support of Julia Jaffal.**

3.2.6 Immunolabeling of Retinal Sections

Immunofluorescence microscopy was performed on semi-thin retinal resin sections obtained from experimental mice injected with myelin oligodendrocyte glycoprotein in complete Freund's adjuvant (MOG/CFA) to induce EAE and control mice injected with CFA alone. This technique provides a precise and reproducible method for analyzing retinal alterations associated with EAE pathology, as previously described (DEMBLA et al., 2018; KESHARWANI et al., 2021; MUKHERJEE et al., 2020). For sample preparation, the eyes were isolated from euthanized mice within 5 minutes post-mortem to preserve tissue integrity. The anterior eyecup, including the cornea, lens, and associated structures, was carefully removed, leaving the posterior eyecup with the attached retina intact. The posterior eyecup was then flash-frozen in liquid nitrogen-cooled isopentane to rapidly preserve cellular and molecular structures. Freeze-drying was carried out in a vacuum chamber using a DUO 004B vacuum pump, maintaining low temperatures with liquid nitrogen cooling for approximately two days. This step ensured optimal preservation of tissue architecture while preparing the samples for resin infiltration (DEMBLA et al., 2018; KESHARWANI et al., 2021; MUKHERJEE et al., 2020; SHANKHWAR et al., 2022; SUIWAL et al., 2022; WAHL et al., 2013). Following lyophilization, samples were gradually equilibrated to room temperature and infiltrated with Epon resin over approximately 48 hours. The infiltration process began with 12 hours of rotation at 28 °C using an overhead rotator operating at 2 rpm to facilitate thorough resin penetration. The process was then continued at room temperature to ensure uniform resin distribution within the tissue. After complete infiltration, the samples were polymerized at 60 °C for two days to produce hardened tissue blocks suitable for sectioning.

Semi-thin sections measuring 0.5 µm in thickness were generated using a Reichert ultramicrotome equipped with a diamond knife. These standardized sections were collected on glass coverslips for further processing. The Epon resin was carefully removed from the sections, preparing them for subsequent immunocytochemistry, as previously described.

For immunolabeling, the sections were double-stained using the indicated primary antibodies at optimized dilutions (see Table 1). The primary antibody incubation was performed overnight at 4 °C to ensure specific binding to the target proteins. In each experiment, reference samples from CFA-injected control mice and experimental samples from MOG/CFA-injected mice were processed simultaneously under identical conditions to ensure comparability.

The next day, sections were washed thoroughly with PBS to remove unbound primary antibodies. They were then incubated with fluorophore-conjugated secondary antibodies (see Table 2) for 1 hour at room temperature. This step enabled the visualization of immunosignals using fluorescence microscopy. Following secondary antibody incubation, the sections were washed multiple times with PBS to

eliminate any unbound antibodies and were subsequently embedded in n-propyl gallate (NPG) antifade solution, which preserves fluorescence signals during imaging (DEMBLA et al., 2018; KESHARWANI et al., 2021; MUKHERJEE et al., 2020; SHANKHWAR et al., 2022; SUIWAL et al., 2022; WAHL et al., 2013). **Experiments were done by Ali El Samad and Julia Jaffal supported experiments.**

3.2.7 Confocal Microscopy and Quantitative Analysis of Immunosignals

Confocal microscopy was employed to analyze immunosignals in retinal sections using a Nikon A1R confocal microscope, following established protocols. High-resolution images were captured with a 60×/1.40 numerical aperture (N.A.) oil objective under the control of NIS Elements software. To ensure consistency across samples, image acquisition for MOG/CFA- and CFA-injected samples was performed under identical settings, utilizing the "re-use image settings" feature of the software. This controlled approach minimized variability introduced by imaging parameters (DEMBLA et al., 2018; DEMBLA et al., 2014; EICH et al., 2017; WAHL et al., 2013; WAHL et al., 2016).

All image acquisition and subsequent analyses were conducted in a blinded manner, with the experimenter unaware of the sample group (CFA or MOG/CFA) to eliminate potential bias. Images of CFA and MOG/CFA samples, derived from each embedding, were captured using the identical re-use option in the software to maintain uniformity in imaging conditions. Each experimental group underwent five independent replicates to ensure robust and reproducible data.

For quantitative analysis, a standardized rectangular region of interest (ROI) was applied to both sample types. The ROI was strategically placed along the outer plexiform layer (OPL), identified unambiguously by distinct actin and EAAT5 immunosignals. ROIs were managed and analyzed using the Analyze-Tools-ROI Manager in ImageJ, a widely used open-source software for image processing. Immunosignals of both EAAT5 and actin were simultaneously recorded to facilitate comparative analysis.

Actin immunosignals served as a reference signal for normalization, as actin expression remained stable and unchanged between CFA- and MOG/CFA-injected samples. This stability makes actin an ideal internal control for correcting potential differences in section thickness or sample preparation. Fluorescence intensities for EAAT5 and actin were measured as integrated density values. EAAT5 intensities were normalized to the corresponding actin values to account for any variability. The arithmetic mean integrated density value for CFA samples was set as the 100% baseline, and the relative values for MOG/CFA samples were expressed as percentages of the CFA baseline.

Quantitative data were compiled and analyzed using Microsoft Excel for initial processing. Statistical analyses were performed with GraphPad Prism 10 (version 10.2.3), a statistical and graphing software, to assess the significance of differences between the experimental groups. These rigorous analytical

procedures ensured accurate and unbiased quantification of immunosignals, providing reliable insights into EAAT5 expression under different experimental conditions.

3.2.8 Statistical Analyses of Immunofluorescence Signals

Statistical analyses were performed using GraphPad 10 (version 10.2.3). Based on prior sample size estimations ($\alpha \leq 0.05$, effect size Cohen's d = 0.8, and power = 0.8) conducted with G*Power Version 3.1.9.6 (FAUL et al., 2007), five independent immunizations were carried out. Each immunization included CFA-injected control animals and MOG/CFA-injected experimental animals, randomly assigned to their respective groups and housed together. Samples for immunofluorescence analysis were randomly selected from these immunizations.

To assess whether data from the individual experiments could be pooled, the consistency of CFA reference group values across experiments was evaluated. The Shapiro–Wilk test was used to check for normal distribution, which was not observed for all datasets. Therefore, Kruskal–Wallis ANOVA followed by Dunn's post hoc test was applied to compare CFA reference groups across experiments. No significant differences were found, allowing data pooling for further analysis.

Pooled data from CFA and MOG/CFA groups were analyzed using the non-parametric Mann–Whitney U test, with significance defined as $p < 0.05$. Post hoc power analysis of the immunofluorescence data yielded a power of 0.985, with an effect size Hedges' g = 0.953835 and $\alpha = 0.0001$(HEDGES, 1981). Statistical analyses were supported by Karin Schwarz.

3.2.9 Western Blot Analysis

The specificity of the EAAT5 antibody was assessed using Western blot (WB) analysis of retinal lysates obtained from wild-type mice. Additionally, the global expression levels of EAAT5 were analyzed and compared between retinal lysates of MOG/CFA-injected EAE mice and CFA-injected control mice.

Retinas were homogenized in ice-cold RIPA lysis. Homogenization was performed using an Ultra Turrax T8A for 1–2 seconds. The retinal lysates were then incubated on ice for 20 minutes with gentle agitation and centrifuged at 13,000 rpm for 30 minutes at 4 °C. The supernatant, containing solubilized proteins, was collected and mixed 1:1 (v/v) with SDS Laemmli buffer, followed by heating at 96 °C for 10 minutes to denature proteins. Protein concentrations were quantified using the Amido Black method (DIECKMANN-SCHUPPERT, SCHNITTLER, 1997), where 5 µL of protein samples and bovine serum albumin (BSA) standards were spotted onto cellulose acetate membranes, air-dried, and stained with Amido Black 10B solution. After washing and drying, the stained membrane pieces were dissolved

in Amido black staining solution. Absorbance at 620 nm was measured with a UV/Visible spectrophotometer and compared to a BSA standard curve to determine protein concentrations.

Thirty micrograms of protein from each retinal lysate were resolved on a 10% acrylamide SDS-PAGE gel. Proteins were electro-transferred onto nitrocellulose membranes at 50 volts for 6.5 hours at 4 °C. Following transfer, membranes were washed with PBS and blocked with 5% (w/v) non-fat dry milk in PBS for 1 hour at room temperature to minimize non-specific binding.

Blocked membranes were incubated overnight at 4 °C with primary antibodies at the optimized dilutions indicated in Table 1. After washing to remove unbound antibodies, membranes were incubated with horseradish peroxidase (HRP)-conjugated secondary antibodies, as specified in Table 2, for 2 hours at room temperature. Excess secondary antibodies were removed by washing three times for 10 minutes each. Antibody binding was visualized using a chemiluminescence detection system (ECL), and signals were imaged using Bio-Rad Gel Doc imaging systems.

To normalize loading variations, membranes were stripped of antibodies using a stripping buffer. Stripping was performed at room temperature with mild shaking for 20 minutes. The membranes were washed with TBST (Tris-buffered saline with 0.1% Tween® 20) to remove residual stripping buffer, re-blocked with 5% (w/v) non-fat dry milk in PBS, and re-probed with a mouse monoclonal anti-actin primary antibody (Table 1). Binding of the actin antibody was visualized using secondary HRP-conjugated antibodies (Table 2) and ECL imaging.

Band chemiluminescence intensity corresponding to EAAT5 expression was quantified using Image Studio Lite software (Li-Cor, version 5.2). A rectangular region of interest (ROI) was defined around the targeted band to measure the corrected pixel intensity sum for area and background. EAAT5 band intensities were normalized to the corresponding actin band intensities within the same lane, as actin levels remained consistent between CFA and MOG/CFA sample.

The normalized EAAT5 band intensity for CFA samples was set to 100%, and values for MOG/CFA samples were expressed relative to this baseline. Data were exported to GraphPad Prism 10 for statistical analysis. Normalized EAAT5 band intensities were normally distributed (Shapiro–Wilk test), and one-sample t-tests were used to assess significant differences, with $p < 0.05$ considered statistically significant. Results were presented as arithmetic means ± standard errors of the mean (S.E.M.), and all individual values were displayed for transparency. **These experiments were supported by Julia Jaffal.**

4 Results

4.1 Validation of the specificity of antigen affinity-purified rabbit polyclonal EAAT5 antibody

This study investigated the expression and distribution of the glutamate transporter EAAT5 in photoreceptor synapses located in OPL of the mouse retina. Using immunofluorescence microscopy, we compared the retinas of MOG/CFA-injected EAE mice with those of CFA-injected control mice, focusing on day 9 post-injection. For immunocytochemical analysis, we employed an antigen-affinity purified rabbit polyclonal antibody specific for EAAT5, validated extensively through both immunolabeling and Western blotting experiments.

The EAAT5 antibody produced prominent punctate immunosignals localized near the presynaptic release sites of photoreceptor synapses in the OPL (Figure 7A1–A3). These presynaptic sites were co-labeled using a mouse monoclonal antibody against RIBEYE (clone 2D9), a principal component of synaptic ribbons (MAXEINER et al., 2016; SCHMITZ et al., 2000; ZENISEK et al., 2004). This co-labeling confirmed the precise localization of EAAT5 immunosignals at synaptic release sites. The punctate pattern of EAAT5 immunoreactivity in the OPL is consistent with previous observations of EAAT5 expression in the mouse retina (GEHLEN et al., 2021). Additionally, we identified punctate EAAT5 immunosignals in the inner plexiform layer (IPL) (Figure 7B1–B3). These signals likely correspond to EAAT5 in the presynaptic terminals of rod bipolar cells, a finding corroborated by earlier studies (GEHLEN et al., 2021).

Specificity of the EAAT5 antibody was further validated through pre-absorption experiments. Pre-incubation of the EAAT5 antibody with the EAAT5 fusion protein, against which the antibody was raised, completely abolished EAAT5 immunosignals in both the OPL and IPL (Figure 7C1–C3, E1–E3). Notably, pre-absorption with an irrelevant HexaHIS-tagged Cre recombinase fusion protein did

not affect EAAT5 immunosignals, confirming that the observed labeling was specific to EAAT5 (Figure 7B1–B3, D1–D3). Importantly, RIBEYE immunosignals remained unaffected under all pre-absorption conditions, further validating the specificity of the EAAT5 antibody.

Western blot analyses provided additional evidence of antibody specificity. The EAAT5 antibody detected the bacterially expressed EAAT5 fusion protein but did not react with the control Cre fusion protein (Figure 7F, G1). The anti-HexaHIS monoclonal antibody was used to confirm the presence of both fusion proteins on the same blot (Figure 7G2). Furthermore, in wild-type mouse retinal lysates, the EAAT5 antibody detected a single protein band at the expected molecular weight of approximately 65 kDa, corresponding to EAAT5 (Figure 7H). Figure 4 was done with the support of Julia Jaffal and Karin Schwarz.
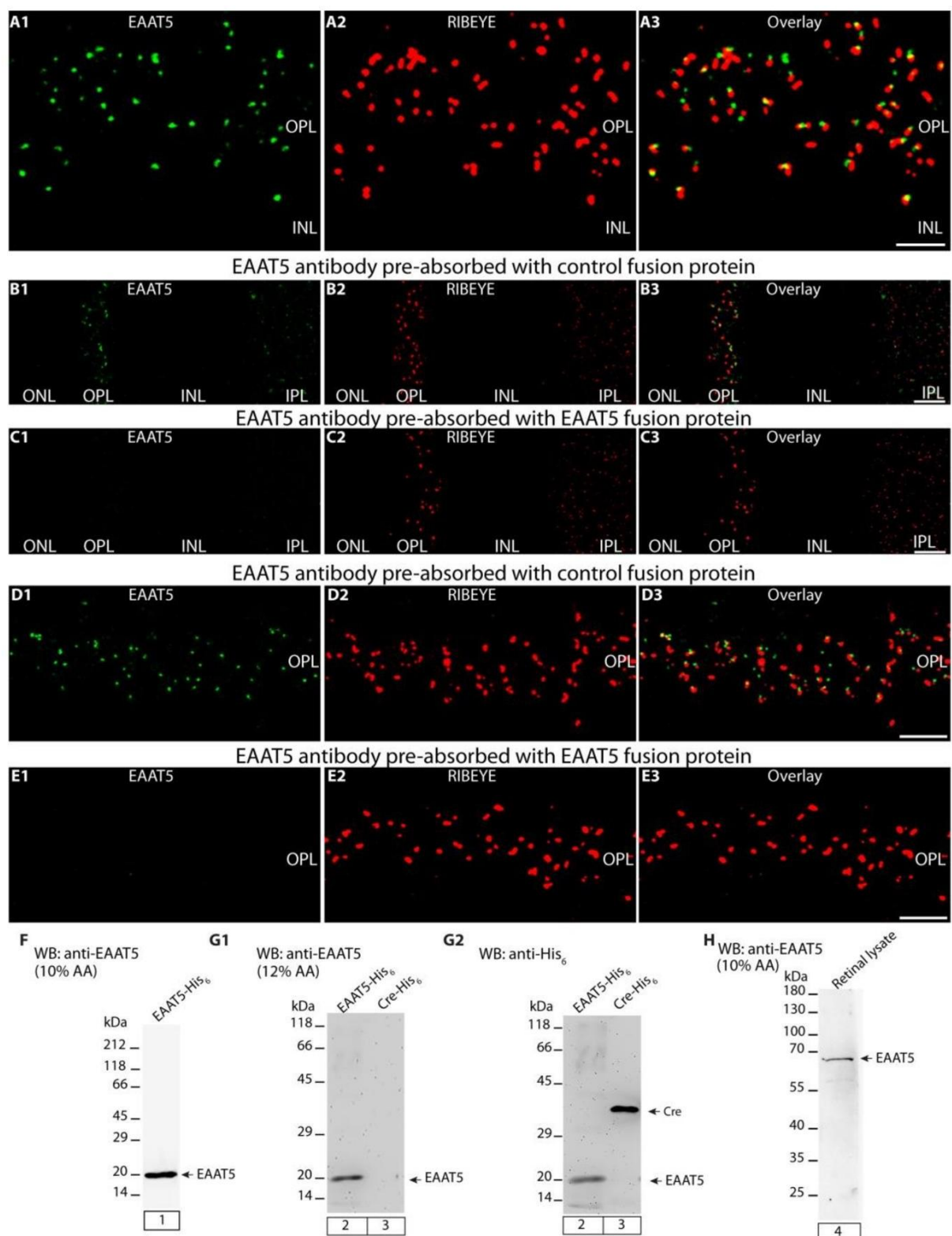
Figure 7. Specificity validation of the antigen affinity-purified EAAT5 antibody. (A1, A2) Magnified images of OPLdouble-immunolabeled with the rabbit polyclonal anti-EAAT5 antibody (green) and the mouse monoclonal anti-RIBEYE antibody (red). (A3) Merged image showing the co-localization of both antibodies at photoreceptor synapses in the OPL. (B1–E3) Pre-absorption experiments on semi-thin (0.5 μm) sections of wild-type mouse retinas. (B1, D1) The EAAT5 antibody pre-absorbed with an unrelated control fusion protein retained immunosignals. (C1, E1) Pre-absorption

with the EAAT5 fusion protein abolished EAAT5 signals. (B2, C2, D2, E2) RIBEYE immunosignals remained unaffected under both conditions. (B3, C3, D3, E3) Merged images combining red and green channels from the respective experiments. (F–H) Western blot analyses confirming EAAT5 antibody specificity. (F, G1) The EAAT5 antibody detected a ~20 kDa band in lanes containing the EAAT5 fusion protein (lanes 1 and 2) but not in the lane with the Cre control fusion protein (lane 3). (G2) Anti-HexaHIS antibody re-probing of the same blot as in (G1) verified the loading of both fusion proteins. (H) A single band at ~65 kDa was observed in wild-type mouse retina lysates, confirming EAAT5 expression. Abbreviations: OPL, outer plexiform layer. Scale bar: 5 μm. Published in (EL SAMAD et al., 2024). Figure from El Samad et al., 2024.
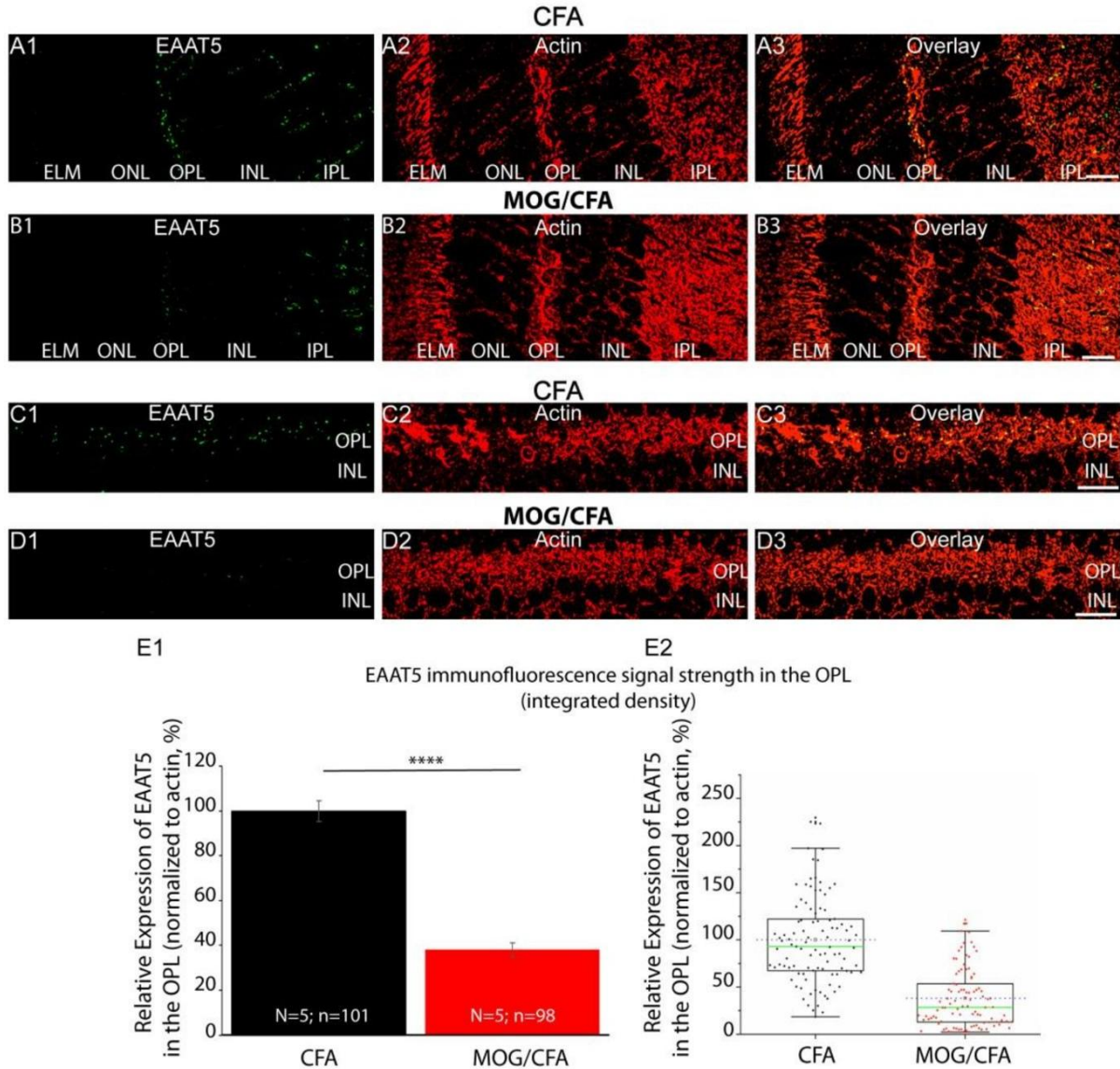
4.2 Immunofluorescence signals of EAAT5 in photoreceptor synapses in OPL of EAE model

We used this validated EAAT5 antibody to compare its expression in the photoreceptor synapses of MOG/CFA-injected EAE mice and CFA-injected control mice by immunohistochemistry. Immunofluorescence microscopy revealed a significant reduction in EAAT5 immunosignals in the OPL of MOG/CFA-injected EAE mice (Figure 8B1-B3, D1-D3 and 9B1–B3, D1–D3) compared to CFA-injected control mice (Figure 8B-B3, D1-D3 9A1–A3, C1–C3). These observations were supported by both qualitative (Figure 8A1-D3 and 9A1–D3) and quantitative (Figure 9E1, E2) analyses. Co-labeling with actin, a reference protein known to remain unchanged at this stage of EAE (DEMBLA et al., 2018), allowed for normalization of EAAT5 immunosignals. Actin labeling also facilitated visualization of the retinal layers, ensuring accurate identification of the OPL and reliable quantification of EAAT5 expression. Negative control images are shown to rule out any autofluorescence or background effect (Figure 8AA4, B4, C4 and D4).
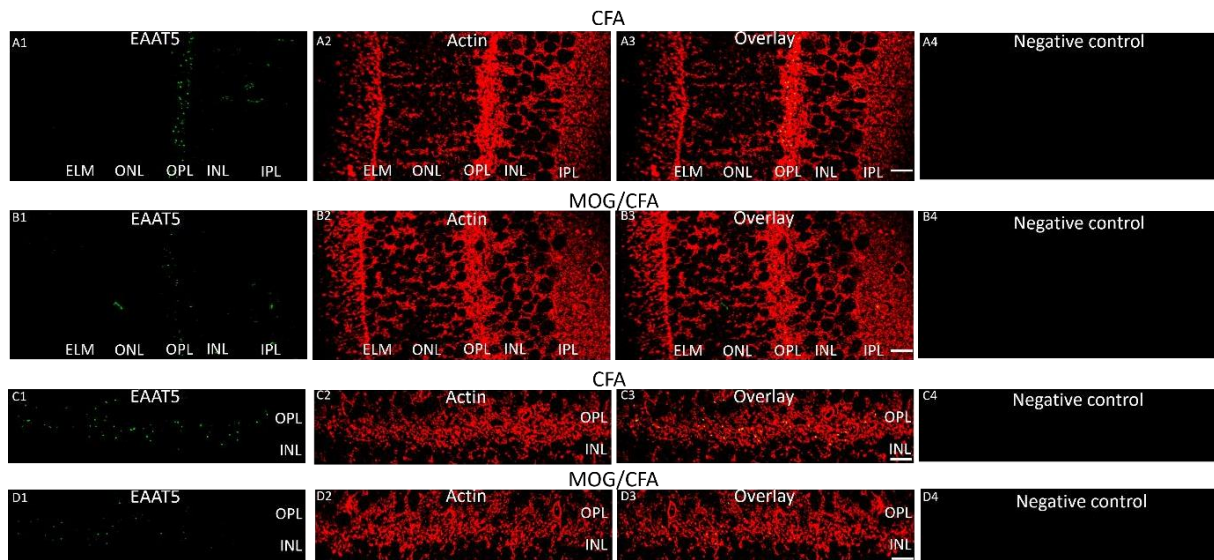
Figure 8. EAAT5 immunofluorescence signals are significantly reduced in photoreceptor synapses in the OPL of MOG/CFA-injected EAE mice compared to CFA-injected control mice. (A1–D3) Double immunolabeling of 0.5 μm-thick retinal sections from CFA-injected control mice and MOG/CFA-injected EAE mice (day 9 post-injection) with a mouse monoclonal antibody against actin (clone C4, red channel) and a rabbit polyclonal antibody against EAAT5 (green channel). Merged images of the red and green channels are shown in (A3, B3, C3, D3). (C1–D3) Magnified views of the

OPL double-labeled with EAAT5 and RIBEYE antibodies. Abbreviations: CFA, complete Freund's adjuvant; EAE, experimental autoimmune encephalomyelitis; MOG, myelin oligodendrocyte protein; N, number of mice; n, number of confocal images analyzed; OPL, outer plexiform layer; S.E.M., standard error of the mean. The negative control panels show the merged green and red channel. Scale bars: 5 μm. Published in (EL SAMAD et al., 2024) Figure from Samad et al., 2024


Figure 9. EAAT5 immunofluorescence signals are significantly reduced in photoreceptor synapses in the OPL of MOG/CFA-injected EAE mice compared to CFA-injected control mice. (A1–D3) Double immunolabeling of 0.5 μm-thick retinal sections from CFA-injected control mice and MOG/CFA-injected EAE mice (day 9 post-injection) with a mouse monoclonal antibody against actin (clone C4, red channel) and a rabbit polyclonal antibody against EAAT5 (green channel). Merged images of the red and green channels are shown in (A3, B3, C3, D3). (C1–D3) Magnified views of the OPL double-labeled with EAAT5 and RIBEYE antibodies. (E1) Histogram showing mean fluorescence intensities (%) of EAAT5 immunosignals in the OPL for CFA and MOG/CFA samples. Data are presented as means ± S.E.M. (****, $p<0.0001$). (E2) Box-and-whisker plot displaying the distribution of individual fluorescence intensity values from (E1), with the mean and median values shown as a dashed blue line and solid green line, respectively. The boxes represent the 25th–75th percentiles, while

the whiskers extend to 1.5 times the interquartile range. Statistical analysis was performed using the Mann–Whitney U test (see Methods, Section 2.3). Abbreviations: CFA, complete Freund's adjuvant; EAE, experimental autoimmune encephalomyelitis; MOG, myelin oligodendrocyte protein; N, number of mice; n, number of confocal images analyzed; OPL, outer plexiform layer; S.E.M., standard error of the mean. Scale bars: 5 μm. Published in (EL SAMAD et al., 2024). Figure from Samad et al., 2024.

4.3 Expression of EAAT5 in the retinal lysates of EAE model

The reduced EAAT5 immunosignals observed in MOG/CFA-injected EAE mice were consistent with findings from Western blot analyses. Global EAAT5 protein expression levels were significantly lower in retinal lysates from EAE mice compared to controls at day 9 post-injection (Figure 10). These reductions highlight the impact of EAE-induced neuroinflammation on EAAT5 expression in the retina. Together, these data provide compelling evidence that EAE disrupts the expression and distribution of EAAT5 in photoreceptor synapses. The reduction in EAAT5 levels in the OPL and IPL of EAE mice suggests that glutamate homeostasis in retinal synapses is compromised, potentially contributing to the synaptic and neuronal dysfunction observed in this model of multiple sclerosis. **This figure was performed with the support and help of Julia Jaffal.**
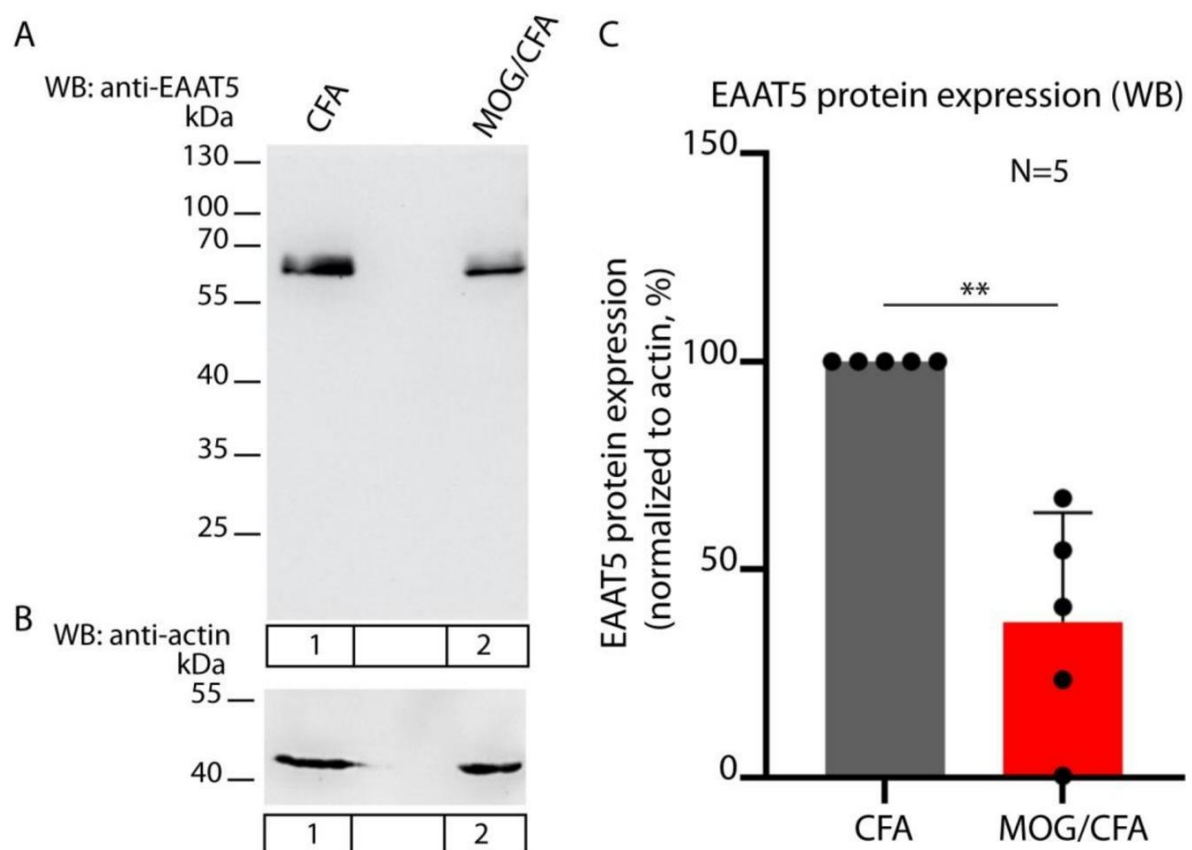
Figure 10. Western blot analysis of total EAAT5 expression in retinal lysates from MOG/CFA-injected EAE mice and CFA-injected control mice at day 9 post-injection. (A) The EAAT5 antibody detects EAAT5 at the expected running position of ~65 kDa in WB analyses of retinal lysates from

CFA-injected control mice and MOG/CFA-injected EAE mice (lanes 1 and 2, respectively). (B) The same WB membrane shown in (A) re-probed with an antibody against actin, which served as a loading control with a band at ~43 kDa. (C) Summary of results from five independent WB experiments analyzing EAAT5 expression in retinas from CFA- and MOG/CFA-injected mice. EAAT5 expression was normalized to actin, and values for the CFA control group were assigned as 100% to highlight relative differences between CFA and MOG/CFA groups. Data in (C) are shown as means ± S.E.M., and statistical significance was determined using a one-sample t-test (**, $p<0.01$). Abbreviations: WB, Western blot; CFA, complete Freund's adjuvant; EAE, experimental autoimmune encephalomyelitis; MOG, myelin oligodendrocyte protein; S.E.M., standard error of the mean; N, number of experiments. Published in (EL SAMAD et al., 2024). Figure from El Samad et al., 2024.

5 Discussion

MS is a chronic neuroinflammatory disease of the CNS characterized by immune dysregulation, demyelination, and axonal degeneration. Elevated levels of pro-inflammatory cytokines, such as TNF-α and IL-1β, are a hallmark of MS and play a pivotal role in disease progression (LEVITE, 2017). These cytokines have been reported to influence the expression and function of glutamate transporters across various CNS regions, resulting in dysregulated glutamate homeostasis (LEE et al., 2017; MANDOLESI et al., 2015; MANDOLESI et al., 2013; PITT et al., 2003; POTENZA et al., 2018; VERCELLINO et al., 2007). Although most studies highlight a cytokine-mediated downregulation of glutamate transporters, some findings indicate an enhanced expression of specific transporters under certain conditions (VALLEJO-ILLARRAMENDI et al., 2006). The association between glutamate transporter polymorphisms and higher glutamate concentrations in relapsing MS further underscores the role of these transporters in MS pathogenesis (BOCCUNI et al., 2023; PAMPLIEGA et al., 2008).

Glutamate transporters are integral to maintaining synaptic glutamate balance by clearing glutamate from the synaptic cleft and preventing excitotoxicity, a pathological process resulting from excessive glutamate levels. Dysfunctional glutamate uptake can cause glutamate spillover from synaptic to extrasynaptic sites, activating extrasynaptic glutamate receptors. This activation triggers neurotoxic cascades, including calcium overload, mitochondrial dysfunction, and oxidative stress, ultimately leading to neuronal and glial cell death (BADING, 2017; FAIRLESS et al., 2021; HARDINGHAM et al., 2001; HARDINGHAM, BADING, 2003, 2010; HARDINGHAM et al., 2002; IZUMI et al., 2002; PARSONS, RAYMOND, 2014; VANDENBERG, RYAN, 2013). Such mechanisms are implicated in the progressive neurodegeneration observed in MS.

This study focused on the presynaptic glutamate transporter EAAT5, localized in photoreceptor and bipolar cell terminals of the retina. EAAT5 is positioned near presynaptic glutamate release sites, which are characterized by the presence of synaptic ribbons, specialized structures that facilitate sustained neurotransmitter release (FYK-KOLODZIEJ et al., 2004; GEHLEN et al., 2021; POW, BARNETT, 2000). The specific role of EAAT5 in modulating synaptic transmission makes it a critical component of retinal glutamate regulation.

Our findings demonstrate a significant downregulation of EAAT5 expression in the photoreceptor synapses of OPLin EAE, a well-established mouse model of MS. Using qualitative and quantitative immunofluorescence microscopy, we observed a marked reduction in EAAT5 immunosignals in MOG/CFA-injected EAE mice compared to CFA-injected controls. Western blot analyses of retinal lysates corroborated these findings, showing a decrease in total EAAT5 protein levels in EAE retinas. The physiological implications of reduced EAAT5 expression in photoreceptor ribbon synapses in EAE remain to be fully elucidated. EAAT5's strategic localization near presynaptic release sites allows it to contribute to the temporal precision of synaptic signaling. Electrophysiological studies have shown that EAAT5 plays a role in feedback inhibition through its glutamate-gated chloride conductance, which helps regulate presynaptic membrane potential (ALLEVA et al., 2022; ARRIZA et al., 1997; CHEN et al., 2021; GEHLEN et al., 2021; LEE et al., 2012; MACHTENS et al., 2015; PALMER et al., 2003; PICAUD et al., 1995; SZMAJDA, DEVRIES, 2011; TSE et al., 2014). This mechanism supports the high temporal resolution required for retinal signal transmission. Impaired EAAT5 function or expression could disrupt this feedback loop, potentially contributing to the decreased visual performance and reduced frequency sensitivity previously reported in EAE mice (DEMBLA et al., 2018).

A critical question arising from these findings is whether reduced EAAT5 expression contributes to glutamate spillover from synaptic to extrasynaptic sites in EAE. EAAT5 has a relatively low capacity for glutamate transport and becomes saturated under conditions of high synaptic activity (BLIGARD et al., 2020; LUKASIEWCZ et al., 2021; TANG et al., 2022; THORESON, CHHUNCHHA, 2023). Thus, its ability to prevent spillover may be limited, particularly under the elevated glutamate release rates associated with EAE. High-capacity glutamate transporters, such as GLAST (EAAT1), are more likely to mitigate glutamate spillover and prevent excitotoxic damage. GLAST, predominantly expressed in Müller glial cells, has been shown to protect retinal ganglion cells from excitotoxicity in EAE (BOCCUNI et al., 2023; POW et al., 2000; RAUEN et al., 1998). Future studies should investigate whether GLAST and other glutamate transporters are similarly affected in photoreceptor synapses during EAE.

6 Outlook

This study highlights significant alterations in the expression of EAAT5, a presynaptic glutamate transporter, in the mouse model of MS. We demonstrated that EAAT5 is significantly downregulated at photoreceptor synapses in the OPL of MOG/CFA-injected EAE mice compared to CFA-injected controls. Given its low-capacity transport properties and localization near presynaptic release sites, EAAT5's reduced expression could impair synaptic signaling and contribute to visual deficits observed in EAE.

EAAT5 is also expressed at retinal bipolar cell terminals, which are structurally and functionally diverse. Whether EAAT5 expression is similarly compromised at bipolar cell synapses in EAE remains to be investigated. The recently developed EAAT5 knockout mouse model provides an excellent tool to explore the functional consequences of EAAT5 dysregulation in retinal and CNS pathologies associated with MS.

Future research should also focus on high-capacity glutamate transporters such as GLAST, which play a critical role in preventing excitotoxic damage. A recent study demonstrated that GLAST is downregulated in the inner retina of EAE mice, and its overexpression via adeno-associated virus (AAV)-mediated gene therapy protected retinal ganglion cells from cell death (BOCCUNI et al., 2023). These findings highlight the therapeutic potential of targeting glutamate transporters in MS. Further exploration of glutamate transport dysregulation in EAE and MS could pave the way for novel neuroprotective strategies to mitigate disease progression and improve patient outcomes.

7 References

1.   (1868) Structure and Function of the Retina. Br Foreign Med Chir Rev 42:329-358
2.   Agathocleous M, Harris WA (2009) From progenitors to differentiated cells in the vertebrate retina. Annu Rev Cell Dev Biol 25:45-69
3.   Aguirre GK, Datta R, Benson NC, Prasad S, Jacobson SG, Cideciyan AV, Bridge H, Watkins KE, Butt OH, Dain AS, Brandes L, Gennatas ED (2016) Patterns of Individual Variation in Visual Pathway Structure and Function in the Sighted and Blind. PLoS One 11:e0164677
4.   Alleva C, Machtens JP, Kortzak D, Weyand I, Fahlke C (2022) Molecular Basis of Coupled Transport and Anion Conduction in Excitatory Amino Acid Transporters. Neurochem Res 47:9-22
5.   Ambrogini P, Torquato P, Bartolini D, Albertini MC, Lattanzi D, Di Palma M, Marinelli R, Betti M, Minelli A, Cuppini R, Galli F (2019) Excitotoxicity, neuroinflammation and oxidant stress as molecular bases of epileptogenesis and epilepsy-derived neurodegeneration: The role of vitamin E. Biochim Biophys Acta Mol Basis Dis 1865:1098-1112
6.   Arriza JL, Eliasof S, Kavanaugh MP, Amara SG (1997) Excitatory amino acid transporter 5, a retinal glutamate transporter coupled to a chloride conductance. Proc Natl Acad Sci U S A 94:4155-4160
7.   Bading H, Segal MM, Sucher NJ, Dudek H, Lipton SA, Greenberg ME (1995) N-methyl-D-aspartate receptors are critical for mediating the effects of glutamate on intracellular calcium concentration and immediate early gene expression in cultured hippocampal neurons. Neuroscience 64:653-664
8.   Bading H (2017) Therapeutic targeting of the pathological triad of extrasynaptic NMDA receptor signaling in neurodegenerations. J Exp Med 214:569-578
9.   Baek JH, Park H, Kang H, Kim R, Kang JS, Kim HJ (2024) The Role of Glutamine Homeostasis in Emotional and Cognitive Functions. Int J Mol Sci 25
10. Baraczka K, Pozsonyi T, Szuts I, Ormos G, Nekam K (2003) Increased levels of tumor necrosis alpha and soluble vascular endothelial adhesion molecule-1 in the cerebrospinal fluid of patients with connective tissue diseases and multiple sclerosis. Acta Microbiol Immunol Hung 50:339-348
11. Benedict RHB, Amato MP, DeLuca J, Geurts JJG (2020) Cognitive impairment in multiple sclerosis: clinical management, MRI, and therapeutic avenues. Lancet Neurol 19:860-871
12. Bezzi P, Domercq M, Brambilla L, Galli R, Schols D, De Clercq E, Vescovi A, Bagetta G, Kollias G, Meldolesi J, Volterra A (2001) CXCR4-activated astrocyte glutamate release via TNFalpha: amplification by microglia triggers neurotoxicity. Nat Neurosci 4:702-710

13. Bligard GW, DeBrecht J, Smith RG, Lukasiewicz PD (2020) Light-evoked glutamate transporter EAAT5 activation coordinates with conventional feedback inhibition to control rod bipolar cell output. J Neurophysiol 123:1828-1837

14. Boccuni I, Fairless R (2022) Retinal Glutamate Neurotransmission: From Physiology to Pathophysiological Mechanisms of Retinal Ganglion Cell Degeneration. Life (Basel) 12

15. Boccuni I, Bas-Orth C, Bruehl C, Draguhn A, Fairless R (2023) Glutamate transporter contribution to retinal ganglion cell vulnerability in a rat model of multiple sclerosis. Neurobiol Dis 187:106306

16. Brandstatter JH, Fletcher EL, Garner CC, Gundelfinger ED, Wassle H (1999) Differential expression of the presynaptic cytomatrix protein bassoon among ribbon synapses in the mammalian retina. Eur J Neurosci 11:3683-3693

17. Bringmann A, Wiedemann P (2012) Muller glial cells in retinal disease. Ophthalmologica 227:1-19

18. Brosnan JT, Brosnan ME (2013) Glutamate: a truly functional amino acid. Amino Acids 45:413-418

19. Buldyrev I, Puthussery T, Taylor WR (2012) Synaptic pathways that shape the excitatory drive in an OFF retinal ganglion cell. J Neurophysiol 107:1795-1807

20. Centonze D, Muzio L, Rossi S, Cavasinni F, De Chiara V, Bergami A, Musella A, D'Amelio M, Cavallucci V, Martorana A, Bergamaschi A, Cencioni MT, Diamantini A, Butti E, Comi G, Bernardi G, Cecconi F, Battistini L, Furlan R, Martino G (2009) Inflammation triggers synaptic alteration and degeneration in experimental autoimmune encephalomyelitis. J Neurosci 29:3442-3452

21. Cepko CL, Austin CP, Yang X, Alexiades M, Ezzeddine D (1996) Cell fate determination in the vertebrate retina. Proc Natl Acad Sci U S A 93:589-595

22. Chen I, Pant S, Wu Q, Cater RJ, Sobti M, Vandenberg RJ, Stewart AG, Tajkhorshid E, Font J, Ryan RM (2021) Glutamate transporters have a chloride channel with two hydrophobic gates. Nature 591:327-331

23. Compston A, Coles A (2008) Multiple sclerosis. Lancet 372:1502-1517

24. Constantinescu CS, Farooqi N, O'Brien K, Gran B (2011) Experimental autoimmune encephalomyelitis (EAE) as a model for multiple sclerosis (MS). Br J Pharmacol 164:1079-1106

25. Costello F (2016) Vision Disturbances in Multiple Sclerosis. Semin Neurol 36:185-195

26. Daghsni M, Aldiri I (2021) Building a Mammalian Retina: An Eye on Chromatin Structure. Front Genet 12:775205

27. De Moraes CG (2013) Anatomy of the visual pathways. J Glaucoma 22 Suppl 5:S2-7

28. Dembla M, Wahl S, Katiyar R, Schmitz F (2014) ArfGAP3 is a component of the photoreceptor synaptic ribbon complex and forms an NAD(H)-regulated, redox-sensitive complex with RIBEYE that is important for endocytosis. J Neurosci 34:5245-5260

29. Dembla M, Kesharwani A, Natarajan S, Fecher-Trost C, Fairless R, Williams SK, Flockerzi V, Diem R, Schwarz K, Schmitz F (2018) Early auto-immune targeting of photoreceptor ribbon synapses in mouse models of multiple sclerosis. EMBO Mol Med 10

30. Dhanapalaratnam R, Markoulli M, Krishnan AV (2022) Disorders of vision in multiple sclerosis. Clin Exp Optom 105:3-12

31. Dieckmann-Schuppert A, Schnittler HJ (1997) A simple assay for quantification of protein in tissue sections, cell cultures, and cell homogenates, and of protein immobilized on solid surfaces. Cell Tissue Res 288:119-126

32. Dobson R, Giovannoni G (2019) Multiple sclerosis - a review. Eur J Neurol 26:27-40

33. Eich ML, Dembla E, Wahl S, Dembla M, Schwarz K, Schmitz F (2017) The Calcineurin-Binding, Activity-Dependent Splice Variant Dynamin1xb Is Highly Enriched in Synapses in Various Regions of the Central Nervous System. Front Mol Neurosci 10:230

34. El Samad A, Jaffal J, Ibrahim DR, Schwarz K, Schmitz F (2024) Decreased Expression of the EAAT5 Glutamate Transporter at Photoreceptor Synapses in Early, Pre-Clinical Experimental Autoimmune Encephalomyelitis, a Mouse Model of Multiple Sclerosis. Biomedicines 12

35. Fairless R, Bading H, Diem R (2021) Pathophysiological Ionotropic Glutamate Signalling in Neuroinflammatory Disease as a Therapeutic Target. Front Neurosci 15:741280

36. Faul F, Erdfelder E, Lang AG, Buchner A (2007) G*Power 3: a flexible statistical power analysis program for the social, behavioral, and biomedical sciences. Behav Res Methods 39:175-191

37. Furukawa T, Ueno A, Omori Y (2020) Molecular mechanisms underlying selective synapse formation of vertebrate retinal photoreceptor cells. Cell Mol Life Sci 77:1251-1266

38. Fyk-Kolodziej B, Qin P, Dzhagaryan A, Pourcho RG (2004) Differential cellular and subcellular distribution of glutamate transporters in the cat retina. Vis Neurosci 21:551-565

39. Gakis G, Angelopoulos I, Panagoulias I, Mouzaki A (2024) Current knowledge on multiple sclerosis pathophysiology, disability progression assessment and treatment options, and the role of autologous hematopoietic stem cell transplantation. Autoimmun Rev 23:103480

40. Gehlen J, Aretzweiler C, Mataruga A, Fahlke C, Muller F (2021) Excitatory Amino Acid Transporter EAAT5 Improves Temporal Resolution in the Retina. eNeuro 8

41. Gibson DG, Young L, Chuang RY, Venter JC, Hutchison CA, 3rd, Smith HO (2009) Enzymatic assembly of DNA molecules up to several hundred kilobases. Nat Methods 6:343-345

42. Green JL, Dos Santos WF, Fontana ACK (2021) Role of glutamate excitotoxicity and glutamate transporter EAAT2 in epilepsy: Opportunities for novel therapeutics development. Biochem Pharmacol 193:114786

43. Grimes WN, Ayturk DG, Hoon M, Yoshimatsu T, Gamlin C, Carrera D, Nath A, Nadal-Nicolas FM, Ahlquist RM, Sabnis A, Berson DM, Diamond JS, Wong RO, Cepko C, Rieke F (2021) A High-Density Narrow-Field Inhibitory Retinal Interneuron with Direct Coupling to Muller Glia. J Neurosci 41:6018-6037

44. Hardingham GE, Arnold FJ, Bading H (2001) Nuclear calcium signaling controls CREB-mediated gene expression triggered by synaptic activity. Nat Neurosci 4:261-267

45. Hardingham GE, Fukunaga Y, Bading H (2002) Extrasynaptic NMDARs oppose synaptic NMDARs by triggering CREB shut-off and cell death pathways. Nat Neurosci 5:405-414

46. Hardingham GE, Bading H (2003) The Yin and Yang of NMDA receptor signalling. Trends Neurosci 26:81-89

47. Hardingham GE, Bading H (2010) Synaptic versus extrasynaptic NMDA receptor signalling: implications for neurodegenerative disorders. Nat Rev Neurosci 11:682-696

48. Hauser SL, Cree BAC (2020) Treatment of Multiple Sclerosis: A Review. Am J Med 133:1380-1390 e1382

49. Hedges LV (1981) Distribution theory for Glass's estimator of effect size and related estimators. journal of Educational Statistics 6:107-128

50. Hendrickson A (2016) Development of Retinal Layers in Prenatal Human Retina. Am J Ophthalmol 161:29-35 e21

51. Hoon M, Okawa H, Della Santina L, Wong RO (2014) Functional architecture of the retina: development and disease. Prog Retin Eye Res 42:44-84

52. Inoue A, Koh CS, Yahikozawa H, Yanagisawa N, Yagita H, Ishihara Y, Kim BS (1996) The level of tumor necrosis factor-alpha producing cells in the spinal cord correlates with the degree of Theiler's murine encephalomyelitis virus-induced demyelinating disease. Int Immunol 8:1001-1008

53. Izumi Y, Shimamoto K, Benz AM, Hammerman SB, Olney JW, Zorumski CF (2002) Glutamate transporters and retinal excitotoxicity. Glia 39:58-68

54. Jasse L, Vukusic S, Durand-Dubief F, Vartin C, Piras C, Bernard M, Pelisson D, Confavreux C, Vighetto A, Tilikete C (2013) Persistent visual impairment in multiple sclerosis: prevalence, mechanisms and resulting disability. Mult Scler 19:1618-1626

55. Johnson PT, Williams RR, Cusato K, Reese BE (1999) Rods and cones project to the inner plexiform layer during development. J Comp Neurol 414:1-12

56. Karali M, Banfi S (2015) Inherited Retinal Dystrophies: the role of gene expression regulators. Int J Biochem Cell Biol 61:115-119

57. Kaur G, Long CR, Dufour JM (2012) Genetically engineered immune privileged Sertoli cells: A new road to cell based gene therapy. Spermatogenesis 2:23-31

58. Kelts EA (2010) The basic anatomy of the optic nerve and visual system (or, why Thoreau was wrong). NeuroRehabilitation 27:217-222

59. Kesharwani A, Schwarz K, Dembla E, Dembla M, Schmitz F (2021) Early Changes in Exo- and Endocytosis in the EAE Mouse Model of Multiple Sclerosis Correlate with Decreased Synaptic Ribbon Size and Reduced Ribbon-Associated Vesicle Pools in Rod Photoreceptor Synapses. Int J Mol Sci 22

60. Kindler E, Trojnar E, Heckel G, Otto PH, Johne R (2013) Analysis of rotavirus species diversity and evolution including the newly determined full-length genome sequences of rotavirus F and G. Infect Genet Evol 14:58-67

61. Korn T (2008) Pathophysiology of multiple sclerosis. J Neurol 255 Suppl 6:2-6

62. Kostic M, Zivkovic N, Stojanovic I (2013) Multiple sclerosis and glutamate excitotoxicity. Rev Neurosci 24:71-88

63. Lau A, Tymianski M (2010) Glutamate receptors, neurotoxicity and neurodegeneration. Pflugers Arch 460:525-542

64. Lee A, Anderson AR, Barnett NL, Stevens MG, Pow DV (2012) Alternate splicing and expression of the glutamate transporter EAAT5 in the rat retina. Gene 506:283-288

65. Lee DH, Seubert S, Huhn K, Brecht L, Rotger C, Waschbisch A, Schlachetzki J, Klausmeyer A, Melms A, Wiese S, Winkler J, Linker RA (2017) Fingolimod effects in neuroinflammation: Regulation of astroglial glutamate transporters? PLoS One 12:e0171552

66. Levite M (2017) Glutamate, T cells and multiple sclerosis. J Neural Transm (Vienna) 124:775-798

67. Liang J, Takeuchi H, Doi Y, Kawanokuchi J, Sonobe Y, Jin S, Yawata I, Li H, Yasuoka S, Mizuno T, Suzumura A (2008) Excitatory amino acid transporter expression by astrocytes is neuroprotective against microglial excitotoxicity. Brain Res 1210:11-19

68. Lublin FD (2005) Clinical features and diagnosis of multiple sclerosis. Neurol Clin 23:1-15, v

69. Lukasiewcz PD, Bligard GW, DeBrecht JD (2021) EAAT5 Glutamate Transporter-Mediated Inhibition in the Vertebrate Retina. Front Cell Neurosci 15:662859

70. Machtens JP, Kortzak D, Lansche C, Leinenweber A, Kilian P, Begemann B, Zachariae U, Ewers D, de Groot BL, Briones R, Fahlke C (2015) Mechanisms of anion conduction by coupled glutamate transporters. Cell 160:542-553

71. Maezawa I, Jin LW, Woltjer RL, Maeda N, Martin GM, Montine TJ, Montine KS (2004) Apolipoprotein E isoforms and apolipoprotein AI protect from amyloid precursor protein carboxy terminal fragment-associated cytotoxicity. J Neurochem 91:1312-1321

72. Magi S, Piccirillo S, Amoroso S, Lariccia V (2019) Excitatory Amino Acid Transporters (EAATs): Glutamate Transport and Beyond. Int J Mol Sci 20

73. Magupalli VG, Schwarz K, Alpadi K, Natarajan S, Seigel GM, Schmitz F (2008) Multiple RIBEYE-RIBEYE interactions create a dynamic scaffold for the formation of synaptic ribbons. J Neurosci 28:7954-7967

74. Mahad DH, Trapp BD, Lassmann H (2015) Pathological mechanisms in progressive multiple sclerosis. Lancet Neurol 14:183-193

75. Malik AR, Willnow TE (2019) Excitatory Amino Acid Transporters in Physiology and Disorders of the Central Nervous System. Int J Mol Sci 20

76. Mandolesi G, Musella A, Gentile A, Grasselli G, Haji N, Sepman H, Fresegna D, Bullitta S, De Vito F, Musumeci G, Di Sanza C, Strata P, Centonze D (2013) Interleukin-1beta alters glutamate transmission at purkinje cell synapses in a mouse model of multiple sclerosis. J Neurosci 33:12105-12121

77. Mandolesi G, Gentile A, Musella A, Centonze D (2015) IL-1beta dependent cerebellar synaptopathy in a mouse mode of multiple sclerosis. Cerebellum 14:19-22

78. Mandolesi G, De Vito F, Musella A, Gentile A, Bullitta S, Fresegna D, Sepman H, Di Sanza C, Haji N, Mori F, Buttari F, Perlas E, Ciotti MT, Hornstein E, Bozzoni I, Presutti C, Centonze D (2017) miR-142-3p Is a Key Regulator of IL-1beta-Dependent Synaptopathy in Neuroinflammation. J Neurosci 37:546-561

79. Matthews G, Fuchs P (2010) The diverse roles of ribbon synapses in sensory neurotransmission. Nat Rev Neurosci 11:812-822

80. Maxeiner S, Luo F, Tan A, Schmitz F, Sudhof TC (2016) How to make a synaptic ribbon: RIBEYE deletion abolishes ribbons in retinal synapses and disrupts neurotransmitter release. EMBO J 35:1098-1114

81. McCarthy DP, Richards MH, Miller SD (2012) Mouse models of multiple sclerosis: experimental autoimmune encephalomyelitis and Theiler's virus-induced demyelinating disease. Methods Mol Biol 900:381-401

82. McCombe PA, Greer JM (2022) Effects of biological sex and pregnancy in experimental autoimmune encephalomyelitis: It's complicated. Front Immunol 13:1059833

83. Mey GM, Mahajan KR, DeSilva TM (2023) Neurodegeneration in multiple sclerosis. WIREs Mech Dis 15:e1583

84. Mitosek-Szewczyk K, Sulkowski G, Stelmasiak Z, Struzynska L (2008) Expression of glutamate transporters GLT-1 and GLAST in different regions of rat brain during the course of experimental autoimmune encephalomyelitis. Neuroscience 155:45-52

85. Mukherjee A, Katiyar R, Dembla E, Dembla M, Kumar P, Belkacemi A, Jung M, Beck A, Flockerzi V, Schwarz K, Schmitz F (2020) Disturbed Presynaptic Ca(2+) Signaling in Photoreceptors in the EAE Mouse Model of Multiple Sclerosis. iScience 23:101830

86. Newcombe J, Uddin A, Dove R, Patel B, Turski L, Nishizawa Y, Smith T (2008) Glutamate receptor expression in multiple sclerosis lesions. Brain Pathol 18:52-61

87. Nicholls DG (2004) Mitochondrial dysfunction and glutamate excitotoxicity studied in primary neuronal cultures. Curr Mol Med 4:149-177

88. O'Brien KM, Schulte D, Hendrickson AE (2003) Expression of photoreceptor-associated molecules during human fetal eye development. Mol Vis 9:401-409

89. Ohgoh M, Hanada T, Smith T, Hashimoto T, Ueno M, Yamanishi Y, Watanabe M, Nishizawa Y (2002) Altered expression of glutamate transporters in experimental autoimmune encephalomyelitis. J Neuroimmunol 125:170-178

90. Palle P, Monaghan KL, Milne SM, Wan ECK (2017) Cytokine Signaling in Multiple Sclerosis and Its Therapeutic Applications. Med Sci (Basel) 5

91. Palmer MJ, Taschenberger H, Hull C, Tremere L, von Gersdorff H (2003) Synaptic activation of presynaptic glutamate transporter currents in nerve terminals. J Neurosci 23:4831-4841

92. Pampliega O, Domercq M, Villoslada P, Sepulcre J, Rodriguez-Antiguedad A, Matute C (2008) Association of an EAAT2 polymorphism with higher glutamate concentration in relapsing multiple sclerosis. J Neuroimmunol 195:194-198

93. Parsons MP, Raymond LA (2014) Extrasynaptic NMDA receptor involvement in central nervous system disorders. Neuron 82:279-293

94. Picaud SA, Larsson HP, Grant GB, Lecar H, Werblin FS (1995) Glutamate-gated chloride channel with glutamate-transporter-like properties in cone photoreceptors of the tiger salamander. J Neurophysiol 74:1760-1771

95. Pitt D, Nagelmeier IE, Wilson HC, Raine CS (2003) Glutamate uptake by oligodendrocytes: Implications for excitotoxicity in multiple sclerosis. Neurology 61:1113-1120

96. Potenza N, Mosca N, Mondola P, Damiano S, Russo A, De Felice B (2018) Human miR-26a-5p regulates the glutamate transporter SLC1A1 (EAAT3) expression. Relevance in multiple sclerosis. Biochim Biophys Acta Mol Basis Dis 1864:317-323

97. Pow DV, Barnett NL (2000) Developmental expression of excitatory amino acid transporter 5: a photoreceptor and bipolar cell glutamate transporter in rat retina. Neurosci Lett 280:21-24

98. Pow DV, Barnett NL, Penfold P (2000) Are neuronal transporters relevant in retinal glutamate homeostasis? Neurochem Int 37:191-198

99. Rahn EJ, Iannitti T, Donahue RR, Taylor BK (2014) Sex differences in a mouse model of multiple sclerosis: neuropathic pain behavior in females but not males and protection from neurological deficits during proestrus. Biol Sex Differ 5:4

100. Raimo S, Santangelo G, Trojano L (2021) The emotional disorders associated with multiple sclerosis. Handb Clin Neurol 183:197-220

101. Rajda C, Pukoli D, Bende Z, Majlath Z, Vecsei L (2017) Excitotoxins, Mitochondrial and Redox Disturbances in Multiple Sclerosis. Int J Mol Sci 18

102. Rao P, Segal BM (2004) Experimental autoimmune encephalomyelitis. Methods Mol Med 102:363-375

103. Rauen T, Taylor WR, Kuhlbrodt K, Wiessner M (1998) High-affinity glutamate transporters in the rat retina: a major role of the glial glutamate transporter GLAST-1 in transmitter clearance. Cell Tissue Res 291:19-31

104. Reese BE (2011) Development of the retina and optic pathway. Vision Res 51:613-632

105. Robinson AP, Harp CT, Noronha A, Miller SD (2014) The experimental autoimmune encephalomyelitis (EAE) model of MS: utility for understanding disease pathophysiology and treatment. Handb Clin Neurol 122:173-189

106. Rodriguez-Campuzano AG, Ortega A (2021) Glutamate transporters: Critical components of glutamatergic transmission. Neuropharmacology 192:108602

107. Rossi S, Motta C, Studer V, Barbieri F, Buttari F, Bergami A, Sancesario G, Bernardini S, De Angelis G, Martino G, Furlan R, Centonze D (2014) Tumor necrosis factor is elevated in progressive multiple sclerosis and causes excitotoxic neurodegeneration. Mult Scler 20:304-312

108. Rovaris M, Barnes D, Woodrofe N, du Boulay GH, Thorpe JW, Thompson AJ, McDonald WI, Miller DH (1996) Patterns of disease activity in multiple sclerosis patients: a study with quantitative gadolinium-enhanced brain MRI and cytokine measurement in different clinical subgroups. J Neurol 243:536-542

109. Sanger GJ, Chang L, Bountra C, Houghton LA (2010) Challenges and prospects for pharmacotherapy in functional gastrointestinal disorders. Therap Adv Gastroenterol 3:291-305

110. Sattler R, Rothstein JD (2006) Regulation and dysregulation of glutamate transporters. Handb Exp Pharmacol:277-303

111. Schmitz F, Konigstorfer A, Sudhof TC (2000) RIBEYE, a component of synaptic ribbons: a protein's journey through evolution provides insight into synaptic ribbon function. Neuron 28:857-872

112. Schmitz F (2009) The making of synaptic ribbons: how they are built and what they do. Neuroscientist 15:611-624

113. Schwarz K, Schmitz F (2023) Synapse Dysfunctions in Multiple Sclerosis. Int J Mol Sci 24

114. Shankhwar S, Schwarz K, Katiyar R, Jung M, Maxeiner S, Sudhof TC, Schmitz F (2022) RIBEYE B-Domain Is Essential for RIBEYE A-Domain Stability and Assembly of Synaptic Ribbons. Front Mol Neurosci 15:838311

115. Shaw PJ, Ince PG (1997) Glutamate, excitotoxicity and amyotrophic lateral sclerosis. J Neurol 244 Suppl 2:S3-14

116. Sheldon AL, Robinson MB (2007) The role of glutamate transporters in neurodegenerative diseases and potential opportunities for intervention. Neurochem Int 51:333-355

117. Shigeri Y, Seal RP, Shimamoto K (2004) Molecular pharmacology of glutamate transporters, EAATs and VGLUTs. Brain Res Brain Res Rev 45:250-265

118. Sterling P, Matthews G (2005) Structure and function of ribbon synapses. Trends Neurosci 28:20-29

119. Stojanovic IR, Kostic M, Ljubisavljevic S (2014) The role of glutamate and its receptors in multiple sclerosis. J Neural Transm (Vienna) 121:945-955

120. Struzynska L, Chalimoniuk M, Sulkowski G (2005) Changes in expression of neuronal and glial glutamate transporters in lead-exposed adult rat brain. Neurochem Int 47:326-333

121. Suiwal S, Dembla M, Schwarz K, Katiyar R, Jung M, Carius Y, Maxeiner S, Lauterbach MA, Lancaster CRD, Schmitz F (2022) Ciliary Proteins Repurposed by the Synaptic Ribbon: Trafficking Myristoylated Proteins at Rod Photoreceptor Synapses. Int J Mol Sci 23

122. Sutton C, Brereton C, Keogh B, Mills KH, Lavelle EC (2006) A crucial role for interleukin (IL)-1 in the induction of IL-17-producing T cells that mediate autoimmune encephalomyelitis. J Exp Med 203:1685-1691

123. Szmajda BA, Devries SH (2011) Glutamate spillover between mammalian cone photoreceptors. J Neurosci 31:13431-13441

124. Tang FS, Yuan HL, Liu JB, Zhang G, Chen SY, Ke JB (2022) Glutamate Transporters EAAT2 and EAAT5 Differentially Shape Synaptic Transmission from Rod Bipolar Cell Terminals. eNeuro 9

125. Thompson AJ, Banwell BL, Barkhof F, Carroll WM, Coetzee T, Comi G, Correale J, Fazekas F, Filippi M, Freedman MS, Fujihara K, Galetta SL, Hartung HP, Kappos L, Lublin FD, Marrie RA, Miller AE, Miller DH, Montalban X, Mowry EM, Sorensen PS, Tintore M, Traboulsee AL, Trojano M, Uitdehaag BMJ, Vukusic S, Waubant E,

Weinshenker BG, Reingold SC, Cohen JA (2018) Diagnosis of multiple sclerosis: 2017 revisions of the McDonald criteria. Lancet Neurol 17:162-173

126. Thoreson WB, Chhunchha B (2023) EAAT5 glutamate transporter rapidly binds glutamate with micromolar affinity in mouse rods. J Gen Physiol 155

127. Tian N (2004) Visual experience and maturation of retinal synaptic pathways. Vision Res 44:3307-3316

128. tom Dieck S, Altrock WD, Kessels MM, Qualmann B, Regus H, Brauner D, Fejtova A, Bracko O, Gundelfinger ED, Brandstatter JH (2005) Molecular dissection of the photoreceptor ribbon synapse: physical interaction of Bassoon and RIBEYE is essential for the assembly of the ribbon complex. J Cell Biol 168:825-836

129. Tse DY, Chung I, Wu SM (2014) Possible roles of glutamate transporter EAAT5 in mouse cone depolarizing bipolar cell light responses. Vision Res 103:63-74

130. Vallejo-Illarramendi A, Domercq M, Perez-Cerda F, Ravid R, Matute C (2006) Increased expression and function of glutamate transporters in multiple sclerosis. Neurobiol Dis 21:154-164

131. van der Feen FE, de Haan GA, van der Lijn I, Huizinga F, Meilof JF, Heersema DJ, Heutink J (2022) Recognizing visual complaints in people with multiple sclerosis: Prevalence, nature and associations with key characteristics of MS. Mult Scler Relat Disord 57:103429

132. Vandenberg RJ, Ryan RM (2013) Mechanisms of glutamate transport. Physiol Rev 93:1621-1657

133. Vercellino M, Merola A, Piacentino C, Votta B, Capello E, Mancardi GL, Mutani R, Giordana MT, Cavalla P (2007) Altered glutamate reuptake in relapsing-remitting and secondary progressive multiple sclerosis cortex: correlation with microglia infiltration, demyelination, and neuronal and synaptic damage. J Neuropathol Exp Neurol 66:732-739

134. Wahl S, Katiyar R, Schmitz F (2013) A local, periactive zone endocytic machinery at photoreceptor synapses in close vicinity to synaptic ribbons. J Neurosci 33:10278-10300

135. Wahl S, Magupalli VG, Dembla M, Katiyar R, Schwarz K, Koblitz L, Alpadi K, Krause E, Rettig J, Sung CH, Goldberg AF, Schmitz F (2016) The Disease Protein Tulp1 Is Essential for Periactive Zone Endocytosis in Photoreceptor Ribbon Synapses. J Neurosci 36:2473-2493

136. Ward M, Goldman MD (2022) Epidemiology and Pathophysiology of Multiple Sclerosis. Continuum (Minneap Minn) 28:988-1005

137. Wasimuddin, Brandel SD, Tschapka M, Page R, Rasche A, Corman VM, Drosten C, Sommer S (2018) Astrovirus infections induce age-dependent dysbiosis in gut microbiomes of bats. ISME J 12:2883-2893

138. Werner P, Pitt D, Raine CS (2000) Glutamate excitotoxicity--a mechanism for axonal damage and oligodendrocyte death in Multiple Sclerosis? J Neural Transm Suppl:375-385

139. Werner P, Pitt D, Raine CS (2001) Multiple sclerosis: altered glutamate homeostasis in lesions correlates with oligodendrocyte and axonal damage. Ann Neurol 50:169-180

140. Wersinger E, Schwab Y, Sahel JA, Rendon A, Pow DV, Picaud S, Roux MJ (2006) The glutamate transporter EAAT5 works as a presynaptic receptor in mouse rod bipolar cells. J Physiol 577:221-234

141. Yi JH, Hazell AS (2006) Excitotoxic mechanisms and the role of astrocytic glutamate transporters in traumatic brain injury. Neurochem Int 48:394-403

142. Zanazzi G, Matthews G (2009) The molecular architecture of ribbon presynaptic terminals. Mol Neurobiol 39:130-148

143. Zenisek D, Horst NK, Merrifield C, Sterling P, Matthews G (2004) Visualizing synaptic ribbons in the living cell. J Neurosci 24:9752-9759

144. Zhou Y, Danbolt NC (2014) Glutamate as a neurotransmitter in the healthy brain. J Neural Transm (Vienna) 121:799-817

145. Zhu JD, Tarachand SP, Abdulwahab Q, Samuel MA (2023) Structure, Function, and Molecular Landscapes of the Aging Retina. Annu Rev Vis Sci 9:177-199

8 List of Figures

9 List of Abbreviation

°C	degree Celsius
AMPA	α-amino-3-hydroxy-5-methyl-4-isoxazolepropionic acid
APS	ammonium persulphate
BSA	bovine serum albumin
CD	cluster of differentiation
CFA	complete Freund's adjuvant
CNS	central nervous system
DMSO	dimethyl sulphoxide
EAATs	excitatory amino acid transporters
EAE	experimental autoimmune encephalitis
EDTA	ethylene diamine tetra-acetic acid
IF	Immunofluorescence
IL	interleukin
MOG	myelin oligodendrocytic glycoprotein
MS	Multiple sclerosis
NMDA	N-Methyl-D-aspartic acid
OCT	optical coherence tomograph
ON	optic neuritis
OPL	outer plexiform layer
PBS	phosphate buffer saline
PBST	phosphate buffer saline-Tween
PCA	Para-hydroxy Coumarin Acid
PTX	pertussis toxin
RGCs	retinal ganglion cells
ROI	region of interest
ROS	reactive oxygen specie
RPE	retinal pigment epitheliu
RT	room temperatur
S.E.M.	standard errors of the mean
SDS	sodium do-decyl sulfate

TNF-α	tumor necrosis factor alpha
WB	Western Blot
Wt	Wild type
μl	microlitre
μM	micromolar
μm	micrometre

10 Publication

El Samad, A*.; Jaffal, J.*; Ibrahim, D.R.; Schwarz, K.; Schmitz, F. Decreased Expression of the EAAT5 Glutamate Transporter at Photoreceptor Synapses in Early, Pre-Clinical Experimental Autoimmune Encephalomyelitis, a Mouse Model of Multiple Sclerosis. *Biomedicines* 2024, *12*, 2545. https://doi.org/10.3390/biomedicines12112545 (* equal contribution)

11 Curriculum Vitae

For data protection reasons, the Curriculum Vitae will not be published in the electronic version of the dissertation.